Title

Optimization of the IPP-bypass mevalonate pathway and fed-batch fermentation for the production of isoprenol in Escherichia coli

Authors

Kang, Aram

Mendez-Perez, Daniel

Goh, Ee-Been

et al.

Publication Date

2019-12-01

DOI

10.1016/j.ymben.2019.09.003

Peer reviewed

Optimization of the IPP-bypass mevalonate pathway and fed-batch fermentation for the production of isoprenol in *Escherichia coli*

Aram Kang[1,2,#], Daniel Mendez-Perez[1,2,#], Ee-Been Goh[1,2], Edward E. K. Baidoo[1,2], Veronica T. Benites[1,2], Harry R. Beller[1,2], Jay D. Keasling[1,2,3,4,5,7], Paul D. Adams[1,3,6], Aindrila Mukhopadhyay[1,2], Taek Soon Lee[1,2,*]

[1]Joint BioEnergy Institute, 5885 Hollis Street, Emeryville, CA 94608, USA.

[2]Biological Systems & Engineering Division, Lawrence Berkeley National Laboratory, Berkeley, CA 94720, USA.

[3]Department of Bioengineering, University of California, Berkeley, CA 94720, USA.

[4]Department of Chemical and Biomolecular Engineering, University of California, Berkeley, CA 94720, USA.

[5]The Novo Nordisk Foundation Center for Biosustainability, Technical University of Denmark, Denmark

[6]Molecular Biophysics & Integrated Bioimaging Division, Lawrence Berkeley National Laboratory, Berkeley, CA 94720, USA.

[7]Center for Synthetic Biochemistry, Institute for Synthetic Biology, Shenzhen Institutes for Advanced Technologies, Shenzhen, China.

[#] These authors contributed equally in this manuscript.

*Corresponding author: Dr. Taek Soon Lee, Joint BioEnergy Institute, 5885 Hollis St. 4th floor, Emeryville, CA 94608, USA; Phone: +1-510-495-2470, Fax: +1-510-495-2629, E-mail: tslee@lbl.gov

Highlights

1. The IPP-bypass pathway was optimized to substantially improve isoprenol titer.
2. PMD mutant was introduced for MVAP conversion with high efficiency.
3. Isoprenol titer reached 3.7 g/L in batch cultures at 44% of the theoretical yield.
4. The highest isoprenol titer (10.8 g/L) was achieved in fed-batch fermentations.
5. Use of a solvent overlay improved titer by removing the toxic final product.

Abstract

Isoprenol (3-methyl-3-buten-1-ol) is a drop-in biofuel and a precursor for commodity chemicals. Biological production of isoprenol via the mevalonate pathway has been developed and optimized extensively in *Escherichia coli*, but high ATP requirements and isopentenyl diphosphate (IPP) toxicity have made it difficult to achieve high titer, yield, and large-scale production. To overcome these limitations, an IPP-bypass pathway was previously developed using the promiscuous activity of diphosphomevalonate decarboxylase, and enabled the production of isoprenol at a comparable yield and titer to the original pathway. In this study, we optimized this pathway, substantially improving isoprenol production. A titer of 3.7 g/L (0.14 g isoprenol per g glucose) was achieved in batch conditions using minimal medium by pathway optimization, and a further optimization of the fed-batch fermentation process enabled an isoprenol titer of 10.8 g/L (yield of 0.105 g/g and maximum productivity of 0.157 g L^{-1} h^{-1}), which is the highest reported titer for this compound. The substantial increase in isoprenol titer via the IPP-bypass pathway in this study will facilitate progress toward commercialization.

Keywords: Isoprenol; IPP-bypass; mevalonate pathway; biofuel; fermentation; bioconversion

1. Introduction

Increasing concerns about the cost and environmental impact of petroleum-derived fuels (Baral et al., 2019) has motivated the development of microbial hosts for the production of fuels from renewable carbon sources (Cheon et al., 2016; Liao et al., 2016; Meadows et al., 2018; Rabinovitch-Deere et al., 2013). In particular, 3-methyl-3-buten-1-ol (isoprenol) is a promising alternative to gasoline due to its anti-knocking properties, comparable energy density, and comparable research octane number (Liu et al., 2014; Mack et al., 2014). Isoprenol is also a precursor for isoprene, a polymer building block used in the production of synthetic rubber (Ye et al., 2016). Production of isoprenol at various levels has been demonstrated in *E. coli* by extensive optimization of the mevalonate (MVA) pathway (George et al., 2015; Li et al., 2018; Zada et al., 2018; Zheng et al., 2013). The conventional MVA pathway includes condensation of three acetyl-CoA molecules and reduction to MVA along with two subsequent phosphorylation reactions by mevalonate kinase (MK) and 5-phosphomevalonate kinase (PMK). The product of phosphorylation, mevalonate diphosphate (MVAPP), is decarboxylated to isopentenyl diphosphate (IPP) by a diphosphomevalonate decarboxylase (PMD). Lastly, isoprenol is formed by hydrolysis of the pyrophosphate group from IPP, and overall these reactions consume 3 mol of ATP per mol of isoprenol.

To overcome intrinsic limitations of the conventional MVA pathway, such as lower pathway efficiency and toxicity of an essential intermediate, IPP, an alternative IPP-bypass MVA pathway (Figure 1A) has been developed by taking advantage of the promiscuous activity of PMD toward the non-native substrate mevalonate monophosphate (MVAP) (Kang et al., 2016). The advantages of this alternative pathway

over the conventional MVA pathway include the prevention of IPP toxicity by avoiding formation of IPP and increased robustness under lower aeration culture conditions, as this new pathway requires less ATP than the original MVA pathway (Kang et al., 2016). In a follow-up study, the PMD was engineered to have higher promiscuous activity towards mevalonate phosphate (MVAP), and isoprenol production was further improved to a titer of 1.2 g/L (Kang et al., 2017).

While previous studies used rich media and small-scale batch fermentations to produce isoprenol, further improvements in yield and productivity using inexpensive media in larger volumes are required in order to derisk trials at commercial scale (Balan, 2014; Hollinshead et al., 2014; Wehrs et al., 2019). In this study we optimize the IPP-bypass mevalonate pathway for production of isoprenol in *E. coli* using several HMGR, HMGS and MK variants as well as engineered PMD mutants to provide optimal levels of the pathway intermediates. As a result of these engineering efforts, isoprenol production in minimal medium reached 3.7 g/L in batch cultures whereas a titer of 10.8 g/L was reached using fed-batch cultures with a solvent overlay in a 2-L bioreactor, which is the highest reported titer for this compound.

2. Materials and Methods

2.1. Plasmids and strains

All plasmids and strains used in this study are listed in Table 1. Strains and plasmids along with their associated information (annotated GenBank-format sequence files) have been deposited in the public version of the JBEI Registry (https://public-registry.jbei.org)

and are physically available from the authors and/or Addgene (http://www.addgene.org) upon request.

2.2. Batch production of isoprenol in *E. coli*

Isoprenol production in EZ-Rich defined medium was performed as previously described (Kang et al., 2016). Briefly, to prepare seed cultures, each single colony was inoculated in LB (lysogeny broth) medium containing appropriate antibiotics and grown overnight. Seed cultures were diluted to an optical density (OD_{600nm}) of 0.05 in EZ-Rich defined medium (Teknova, USA) supplemented with 10 g/L glucose (1 %, w/v) and two antibiotics, namely, 100 μg/mL ampicillin and 30 μg/mL chloramphenicol. Diluted cell cultures (5 mL) were first grown at 37°C with shaking at 200 rpm. When cell density reached an OD_{600nm} value of 0.4-0.6, expression of proteins was induced with 0.5 mM IPTG, and the cultures were transferred to an incubator at 30°C with shaking at 200 rpm. Isoprenol production in defined minimal media was performed with M9-MOPS minimal medium (M9 medium (33.9 g/L Na_2HPO_4, 15 g/L KH_2PO_4, 5 g/L NH_4Cl, 2.5 g/L NaCl) supplemented with 75 mM MOPS, 2 mM $MgSO_4$, 1 mg/L thiamine, 10 nM $FeSO_4$, 0.1 mM $CaCl_2$, and micronutrients including 3×10^{-8} M $(NH_4)_6Mo_7O_{24}$, 4×10^{-6} M boric acid, 3×10^{-7} M $CoCl_2$, 1×10^{-7} M $CuSO_4$, 8×10^{-7} M $MnCl_2$, and 1×10^{-7} M $ZnSO_4$) with glucose (10-30 g/L, depending on production conditions) as a sole carbon source.

Strains used for production in minimal medium were first adapted in the medium by serially diluting cell cultures in fresh minimal medium. Briefly, each single colony was inoculated in LB overnight and diluted 50-fold (v/v) in M9-MOPS minimal medium. Cultures were grown for another 24 h and re-diluted 50-fold (v/v) in fresh M9-MOPS

medium. These steps were repeated four times, and the final cell cultures adapted to M9-MOPS medium were stored as frozen glycerol stocks at -80°C. For batch production, a loopful of glycerol stock was inoculated in 2 mL M9-MOPS minimal medium with 1% glucose, and seed cultures were grown overnight at 37°C with shaking at 200 rpm and diluted 50-fold in 5 mL M9-MOPS medium with appropriate antibiotics and glucose at concentrations indicated.

2.3. Isoprenol production in fed-batch fermenter

Fed-batch fermentation was performed in a 2-L bioreactor (Sartorius BIOSTAT B plus) with control for dissolved oxygen (DO), pH, and temperature. A 5-mL culture was inoculated from a frozen glycerol stock, grown for 24 hours, and then used to inoculate a 50-mL culture in a 250-mL flask; this culture was then used to inoculate the bioreactor to an OD_{600nm} of 0.1. The medium for batch phase was M9 minimal medium supplemented with 2 mM $MgSO_4$, 1 mg/L thiamine, 10 µM $FeSO_4$, 0.1 mM $CaCl_2$, additional NH_4Cl (if needed), glucose (2% or 3% w/v), 10 g/L yeast extract (if needed), appropriate antibiotics and micronutrients including 3×10^{-8} M $(NH_4)_6Mo_7O_{24}$, 4×10^{-6} M boric acid, 3×10^{-7} M $CoCl_2$, 1.5×10^{-7} M $CuSO_4$, 8×10^{-7} M $MnCl_2$, and 1×10^{-7} M $ZnSO_4$. The pH of the culture was maintained at 7.0 by supplementation with a base solution (10 N KOH). Temperature, DO, and airflow were set to 30°C, 30%, and a rate of 1 VVM (volume of air per volume of liquid per minute), respectively, throughout the fermentation run. Protein expression was induced with 0.5 mM IPTG when the culture reached an OD_{600nm} of 0.4-0.6. Glucose feeding started when the initial amount of glucose was depleted (indicated by a sharp increase in DO or HPLC analysis) with a feed solution containing

200 g/L glucose, 15 g/L $MgSO_4 \cdot 7H_2O$, 5 g/L yeast extract (if needed), micronutrients according to previous descriptions (Korz et al., 1995) and appropriate antibiotics; also, antifoam B was added to the bioreactor when required. Glucose feeding was carried out using a Watson-Marlow DU520 peristaltic pump; for constant feeding, the flow rate was selected to closely match the glucose consumption rate at the end of the batch phase. For exponential feeding, the feeding rate was changed every hour (for a total of 12 hours) and calculated according to the following equation (Korz et al., 1995):

$$m(t) = \left(\frac{\mu}{Y_{X/S}} + m\right) V_{t_F} X_{t_F} e^{\mu(t-t_F)},$$

where $m(t)$ is the mass flow of the substrate (g/h), μ is the specific growth rate (0.1 h^{-1}), $Y_{X/S}$ is the biomass/substrate yield coefficient (0.5 g/g), m is the specific maintained coefficient (0.025 g g^{-1} h^{-1}), V_{tF} is the cultivation volume at the time of feeding (t_F) and X_{tF} is the biomass concentration (g/L). After 12 hours of exponential feeding, the feeding rate was set constant and glucose was continuously measured in the medium, and the feeding rate was adjusted to prevent its accumulation at more than 2 g/L. For the two-phase cultivation, 20% (v/v) oleyl alcohol was added to the fermenter at the time of induction. During the fed-batch phase, additional oleyl alcohol was added so its volume never decreased below 10% of the total volume. For OD_{600nm} measurement and isoprenol quantification during the two-phase cultivation, the sample was first separated by centrifugation (8 min, 4000 x *g*) and the aqueous phase was used to quantify isoprenol as described above (except that up to 1:3 dilutions with ethyl acetate were used for isoprenol concentrations greater than 2 g/L) as well as OD_{600nm} and DCW (dry cell weight) measurements; in order to quantify isoprenol from the organic phase, 10 µL of the oleyl alcohol was added to 990 µL ethyl acetate containing 1-butanol as an internal standard

and the total isoprenol was calculated based on the actual culture volume at the time of the sampling.

2.4. Isoprenol quantification by gas chromatography (GC)

For isoprenol quantification, an aliquot of cell culture (250 µL) was combined with an equal volume of ethyl acetate (250 µL) containing 1-butanol (30 mg/L) as an internal standard and vigorously mixed for 15 min. Mixtures of cell cultures and ethyl acetate were centrifuged at 20,000 x *g* for 3 min, and 50 or 100 µL of the ethyl acetate layer was diluted 10-fold or 5-fold in ethyl acetate containing 1-butanol (30 mg/L). An aliquot (1 µL) of each of the diluted samples was analyzed by gas chromatography – flame ionization detection (Thermo Focus GC) equipped with a DB-WAX column (15-m, 0.32-mm inner diameter, 0.25-µm film thickness, Agilent, USA), the oven temperature program was as follows: started at 40°C, a ramp of 15°C/min to 100°C, a ramp of 40°C/min to 230°C and held at 230°C for 3 min.

2.5. Quantification of metabolites, sugars and fermentation acids.

For analysis of metabolites from the IPP-bypass pathway, 0.5-1 mL of cell culture was centrifuged at 14,000 x *g* for 3 min at 4°C, the cell pellets were resuspended in 250 µL of methanol and stored at 20°C. Pellets were thawed on ice and combined with 250 µL water, the methanol-water mixtures were centrifuged at 15,000 rpm for 10 min at 4°C and the supernatant was filtered through a Millipore™ Amicon Ultra 3kD MW cut-off filter at 14,000 x *g* for 45 min at 4°C. Filtered solutions were diluted with an equal volume of acetonitrile (final 50% (v/v) ACN) and analyzed via liquid chromatography-mass

spectrometry (LC-MS; Agilent Technologies 1200 Series HPLC system and Agilent Technologies 6210 time-of-flight mass spectrometer) on a ZIC-HILIC column (150-mm length, 4.6-mm internal diameter, and 5-µm particle size) (Baidoo et al., 2019). Concentrations of intracellular metabolites were calculated assuming cell volume of 1 OD_{600nm} /mL as 3.6 µL (Volkmer and Heinemann, 2011).

For quantification of glucose and organic acids, 5 µL of filtered supernatant (0.45-µm centrifugal filter) was analyzed by isocratic elution with 4 mM sulfuric acid through an HPLC system equipped with an Aminex HPX-87H column (Bio-Rad, Richmond, CA, USA) and a refractive index detector (Agilent Technologies). The sample tray and column compartment were set to 4 and 50°C, respectively, and the flow rate was maintained at 0.6 mL/min. Data acquisition and analysis were performed via Chemstation software (Agilent Technologies).

3. Results and Discussion

3.1. Pathway optimization for the biosynthesis of MVAP

For isoprenol production via the IPP-bypass mevalonate pathway, we initially expressed *atoB* (*E. coli*), *HMGS_Sc_o* (*S. cerevisiae*), *HMGR_Sc_o* (*S. cerevisiae*) and *MK_Sc_co* (*S. cerevisiae*, codon optimized) from a medium-copy plasmid and the PMD (*S. cerevisiae*) from a high-copy plasmid (Kang et al., 2016) (plasmid arrangements are shown in Figure 1B); isoprenol production reached 513 mg/L after 48 hours using EZ-Rich medium supplemented with 1% glucose (strain AK01, Figure 2A). Using this strain as a baseline, we tested different expression levels of MK, HMGR, and HMGS in order to identify limiting steps for the biosynthesis of MVAP in the IPP-bypass pathway.

First, we tested whether increasing the expression of the MK would affect isoprenol production. We expressed MK (i.e., *MK_Sc_co*) from a high-copy plasmid (ColE1-origin) with a Trc promoter instead of the medium-copy plasmid (p15A origin, Figure 1C), which increased the isoprenol titer significantly, reaching 1.05 g/L (strain AK02, Figure 2A), suggesting that isoprenol production might be limited by MVAP levels. To test whether the changes in expression of the enzymes upstream of the MK such as HMGS and HMGR would also improve isoprenol production, we tested variants of these enzymes from different organisms (Table 1). The three HMGS variants tested were from *S. cerevisiae* (*HMGS_Sc_o*, native sequence; and *HMGS_Sc_co*, codon-optimized sequence) and from *S. aureus* (*HMGS_Sa*), and the five HMGR variants tested were from *S. cerevisiae* (*HMGR_Sc_co*, codon-optimized), *S. aureus* (*HMGR_Sa*), *Bordetella petrii* (*HMGR_Bp*), *Delftia acidovorans* (*HMGR_Da*), and *Pseudomonas mevalonii* (*HMGR_Pm*) (Ma et al., 2011). Both the HMGR_Sc_co and HMGR_Sa use NADPH as co-factor and have preference for the forward reaction (conversion of HMG-CoA to mevalonate), whereas the HMGR_Bp, HMGR_Da and HMGR_ Pm preferentially use NADH as cofactor (Ma et al., 2011). Different combinations of the HMGS and HMGR variants were tested while *MK_Sc_co* was expressed from the high copy plasmid. Figure 2B shows that isoprenol production was improved when the HMGR_Sc_co and HMGS_Sc_co were used (1.34 g/L, strain AK07) and when HMGR_Sa was used in combination with either the HMGS_Sc_co (1.35g/L, strain AK08) or HMGS_Sa (1.26 g/L, strain AK09). In general, lower isoprenol levels were observed when the NADH-dependent HMGRs were used; since these HMGRs have relatively higher activity for the reverse reaction (conversion of mevalonate to HMG-CoA) (Ma et al., 2011), it is possible

that less carbon flux is being directed to the formation of mevalonate and downstream intermediates. Higher isoprenol titers were observed when the MK_Sc_co and the HMGRs with higher forward reaction activity were overexpressed, which suggests that production of isoprenol could be limited by the availability of mevalonate and mevalonate phosphate (MVAP). Several MK variants were also tested but titers were not improved (Figure 2C). We also tested if higher HMGR expression would positively affect carbon flux towards mevalonate as HMGR is known as a rate-limiting enzyme of the top pathway (acetyl-Co to mevalonate), but expression of an additional copy of the HMGR from a high-copy plasmid did not improve titers either (Figure 1D); in fact, a decrease in isoprenol production was observed compared to the control strain regardless of the HMGR variant used (Figure 2D). Further analysis of one of these HMGR-overexpressing strains (strain AK19) showed that expression of this additional enzyme from the high-copy plasmid resulted in a lag phase after induction (Supplementary Figure 1A), which indicates that growth of the strain was inhibited; the growth recovered after 40 hours but this increase in cell biomass did not result in an increase of isoprenol production (Supplementary Figure 1B). Quantification of intermediate metabolites showed an increase in MVAP levels when the additional HMGR was expressed but no accumulation of other potentially toxic intermediates was observed (Supplementary Figure 1C). We also tested whether overexpression of the HMGR itself was toxic to the cells, but overexpression of only the HMGR_Sc_co from a pTrc promoter from a high-copy number plasmid did not inhibit growth (data not shown).

3.2. Pathway optimization with PMD mutants

Based on the results from the previous section, we hypothesized that the conversion of MVAP to IP might also be a bottleneck in the pathway. Therefore, in order to improve the conversion of MVAP to IP, we tested a PMD mutant (R74G) that was reported to have higher K_i than the wild-type PMD (MVAP is a non-competitive inhibitor of PMD) (Kang et al., 2017). Initially, both the wild-type PMD (strain AK07) and the R74G mutant (strain AK21) were expressed with enzyme variants described in the previous section containing the HMGS_Sc_co, HMGR_Sc_co, and MK_Sc_co. The maximum isoprenol titers of two strains were similar, but there was a significant improvement in rate of production with the R74G mutant (strain AK21) compared to the wild-type PMD (strain AK07), reaching a maximum titer of 1.6 g/L after 30 hours instead of 40 hours (Figure 3A). The strain AK21 also showed faster growth (Figure 3B) and faster glucose consumption (Supplementary Figure 2A). Acetate accumulation peaked at 6 hours after induction reaching 0.8 g/L in both strains, but it decreased to 0.5 g/L and 0.3 g/L in the AK07 and AK21 strains, respectively, at 30 hours after induction (Supplementary Figure 2B). Slower assimilation of acetate for strain AK07 might explain the slower glucose consumption rate at the early stage after induction. In order to test how the use of the R74G PMD mutant affected the conversion of MVAP, we measured MVA, MVAP and IP over time (Figure 3B). Both the intracellular and extracellular concentrations of MVAP were significantly lower in the strain with the R74G mutant (strain AK21) compared to those of the strain with the wild-type PMD (strain AK07), whereas the IP levels were higher, suggesting that using the R74G mutant increases the conversion of MVAP to IP. The strain AK21 also showed lower mevalonate concentrations, suggesting that mevalonate was converted to MVAP more efficiently in strain AK21 than in strain

AK07, where mevalonate increased over time and reached a final concentration four times higher than in strain AK21 after 24 hours (Figure 3B).

In addition to the R74G mutant, two other PMD mutants with higher k_{cat} or higher K_i for MVAP were identified in our previous study, and these mutants could increase the conversion efficiency of MVAP to IP and improve isoprenol production (Kang et al., 2017); one contains a single R74H mutation and the other contains three mutations, R74H, R147K and M212Q (abbreviated as HKQ). The PMD with these mutations were also tested with the HMGS_Sc_co-HMGR_Sc_co-MK_Sc_co system (strains AK22 and AK23, respectively) but lower isoprenol titers were observed (Figure 4A). We hypothesized that other HMGS, HMGR, and MK variants could provide different metabolite levels for the upstream intermediates, which could have synergistic effects on isoprenol production for the PMD mutants. Therefore, two additional strains containing the HMGS_Sa-HMGR_Sa-MK_mm or the HMGS_Sa-HMGR_Sa-MK_Sc_co (which showed high isoprenol titers in the previous section) were also tested with the PMD mutants (Figure 4A). Interestingly, very different isoprenol titers were observed for each PMD mutant depending on the HMGS-HMGS-MK system used; these differences were more significant with the R74H mutant, where the titer ranged from 784 mg/L for strain AK22 to 1.84 g/L for strain AK28 (Figure 4A). In general, higher titers were observed using the HMGS_Sa-HMGR_Sa-MK_Sc_co system, reaching a maximum titer of 1.84 g/L with the R74H mutant (strain AK28) and 1.81 g/L with the HKQ mutant (strain AK29).

3.3. Isoprenol production in minimal media

Because of its greater batch-to-batch consistency and lower cost, chemically defined minimal medium is usually employed for production in bench-scale fermentations; however, since all metabolites need to be synthesized *de novo*, growth in minimal medium can result in major shifts in cell resources and affect production (Singh et al., 2017). Therefore, we tested our previously optimized strains for production on minimal medium supplemented with 1% glucose; isoprenol production was approximately half of that obtained with rich medium (Supplementary Figure S3). Increasing the glucose concentration to 2% generally resulted in higher titers, except for a few strains (e.g., AK28 and AK29), but the degree of improvement varied depending on the MK, HMGS, HMGR, and PMD variants used (Figure 4B). In general, strains with lower isoprenol production showed slower growth and higher acetate accumulation (data not shown). The highest isoprenol titer was achieved when the R74G PMD mutant was expressed with the HMGS_Sc_co-HMGR_Sc_co-MK_Sc_co system (strain AK21), reaching titers of 2.74 g/L. Comparable titers were also observed with strains AK27, AK25 and AK26. Interestingly, more than a 10-fold difference in isoprenol titer was observed for the R74G mutant depending on the HMGS-HMGR-MK system used (ranging from 246 mg/L for strain AK24 to 2.74 g/L for strain AK21; Figure 4B). The initial glucose concentration affected not only the titer but also the yield; for example, for strain AK26, the yield from 1% glucose was 0.095 g isoprenol per g glucose, whereas from 2% glucose the yield was 0.14 g isoprenol per g glucose; the latter is close to 44% of the theoretical yield using the MVA pathway (Dugar and Stephanopoulos, 2011). In both cases, the stationary phase was reached after 20 hours (Figure 5A), therefore, it is possible that the higher yield with 2% glucose was due to additional isoprenol produced during stationary phase when

production could occur without cell growth. The glucose consumption rates of AK26 in minimal medium supplemented with 2% glucose were slower (0.37 g glucose per hour) than those in the medium with 1% glucose (0.49 g glucose per hour; Figure 5B), but there was no significant difference in the isoprenol production rate or biomass production estimated by OD_{600nm} while glucose was being consumed (Figure 5C). Although both the glucose consumption and isoprenol accumulation increased linearly until the glucose was fully consumed, it is interesting to note that no increase in growth (OD_{600nm}) was observed after 22 hours regardless of the initial glucose concentration. This halted growth could be due to a limiting nutrient or the accumulation of growth inhibitors in the medium. After biomass production stopped at ~ 22 hr, isoprenol yield did not increase, suggesting that a portion of the remaining glucose was used for byproduct formation (e.g., acetate and ethanol): both fermentation byproducts showed a gradual increase during stationary phase, when ethanol accumulated to 1.2 g/L (Supplementary Figure S4). Three of the strains with the highest titers (AK21, AK26 and AK27) were further tested for production using minimal medium supplemented with 3% glucose (Figure 6). Interestingly, a significant improvement in titer was observed for strain AK26, reaching 3.71 g/L of isoprenol after 63 hours (Figure 6A), but not for strains AK27 and AK21. A higher glucose consumption rate and less acetate accumulation were observed for strain AK26, which might explain the difference in titers (Figure 6B and 6C). The yield for strain AK26 using 3% glucose was the same as when 2% glucose was used (0.14 g isoprenol per g glucose), whereas ethanol accumulated to 1.9 g/L (Figure 6D) and acetate was not produced at significant levels (0.3 g/L, Figure 6B). Since the mevalonate pathway generates 6 mol of NADH per mol of isoprenol produced (Dugar and

Stephanopoulos, 2011), accumulation of ethanol suggests that glucose might be used for production of ethanol to regenerate NAD^+ from excessive accumulation of NADH generated as a result of higher isoprenol production. When the glucose concentration was further increased to 4% and 5%, lower isoprenol titers, lower glucose consumption rate, and significant acetate accumulation were observed (data not shown), which is a signature feature of overflow metabolism (Basan et al., 2015; Szenk et al., 2017; Wolfe, 2005).

3.4. Fed-batch fermentation

3.4.1. Media and feeding optimization

To test if higher titers and yields of isoprenol could be achieved in a bioreactor by feeding additional glucose, the optimized strain presented in the previous section (strain AK26) was used for fed-bath fermentations in a 2-L bioreactor. M9 minimal medium with 2% glucose (see Material and Methods for full description of the medium components) was used during the batch phase, and glucose was continuously added at a constant rate when the initial glucose was depleted, indicated by a sharp increase in DO or by HPLC analysis of the glucose level. This initial fermentation is referred to as Ferm 1 and subsequent fermentations are numbered accordingly (for a description of all cultivation conditions and a summary of titers, yields, and productivities, see Supplementary Table S1). Figure 7A shows that production of isoprenol for Ferm 1 continuously increased during the fermentation, reaching a titer of 3.55 g/L and a yield of 0.048 g/g glucose at 150 hours, which is lower than what we observed under shake flask-conditions (yield of 0.14 g/g glucose). The growth profile of Ferm 1 (Figure 7B) showed

that the OD_{600nm} reached 6.2 at 22 hours and that the glucose in the batch medium was depleted after 48 hours of cultivation (Supplementary Figure S5). This result suggests that growth was halted even before all glucose was consumed. Therefore, we hypothesize that nutrients other than glucose might be limiting growth during the batch phase. When we increased the concentration of the nitrogen source (NH_4Cl) in the batch medium, from a C/N ratio of 18 in Ferm 1 to a ratio of 10 (Ferm 2), a maximum OD_{600nm} of 7.5 was reached at 22 hours (see Ferm 2 in Figure 7B). Also, there was a significant reduction in the time needed for the complete consumption of the initial glucose in the batch culture from 55 hours to 30 hours (see Supplementary Figure S5), reflecting a higher glucose consumption rate for Ferm 2 compared to that of Ferm 1. Despite the higher biomass accumulation during the batch phase, the maximum isoprenol titer for Ferm 2 was 3.44 g/L at 119 hours, which is similar to that of Ferm 1 (Figure 7A).

Instead of feeding glucose at a constant rate, more efficient feeding strategies have been developed in order to prevent overfeeding or underfeeding of the substrate; in particular, feeding the limiting substrate at an exponentially increasing rate results in constant specific growth rates (Korz et al., 1995). Therefore, we changed the feeding strategy from constant feeding to exponential feeding (see Materials and Methods for details). As shown in Figure 7B the exponential feeding strategy (Ferm 3) resulted in a continuous increase in OD_{600nm} during the first 50 hours of the fermentation (c.f. batch phase ended ca. 30 hours), a maximum OD_{600nm} of 11.1, and a significant increase in isoprenol titer, reaching a maximum titer of 4.86 g/L.

It has been shown that *E. coli* growth on minimal medium containing ammonium salts as a sole nitrogen source can be significantly improved by supplementing the medium with

an organic nitrogen source such as yeast extract, as it provides amino acids that can be directly used for enzyme synthesis (Hugo and Lund, 1968). Therefore, we supplemented the cultivation medium with yeast extract (10 g/L in the batch phase and 5 g/L during the fed-bath phase) to test its effect on growth and production of isoprenol. As can be seen in Figure 7B (Ferm 4), supplementing the medium with yeast extract resulted in higher OD values compared to previous fermentations, reaching a maximum OD_{600nm} of 16.7. Moreover, the isoprenol titer also improved, reaching a maximum of 5.42 g/L after 94 hours. Since exponential feeding and the addition of yeast extract (which constituted less than 10% of the total carbon added) resulted in significant improvements in OD_{600nm} and titer, these conditions were used for further fermentations.

3.4.2. Reduction of acetate formation

During the optimization of the medium and feeding strategy, it was observed that the OD_{600nm} of the culture decreased after 46 hours (see Ferm 4 in Figure 7B), and a significant amount of acetate (1.5 g/L) was observed at 54 hours; acetate concentration continued to increase to more than 6.6 g/L by the end of the fermentation (see Ferm 4 in Figure 8A). Acetate accumulation not only represents a loss of carbon but it can also be detrimental to cell growth at concentrations as low as 1 g/L, affecting the stability of intracellular proteins and acting as proton conductor that can reduce proton motive force (Eiteman and Altman, 2006; De Mey et al., 2007). Two main pathways are responsible for acetate production in *E. coli*, the pyruvate oxidase and the acetate kinase - phosphotransacetylase pathway, which are encoded by the *poxB* and *ackA/pta* genes, respectively (see Figure 1A). To minimize acetate production during the fermentation, a

418 strain in which these acetate-pathway genes were deleted (strain AK30) was used for
419 isoprenol production in the fermenter. No acetate was detected during the fermentation
420 when this mutant strain was used (Ferm 5, Figure 8A); moreover, there was no significant
421 decrease in OD_{600nm} during the cultivation as was previously observed for the wild-type
422 strain (Ferm 4, Figure 7B).
423 The glucose consumption rate for the mutant strain was similar to that of the wild-type
424 strain (Figure 8D) but the isoprenol titer increased 14%, reaching 6.15 g/L after 95 hours
425 (Figure 8C). This result suggests that removal of acetate pathway prevented the loss of
426 carbon to acetate, improving the conversion of glucose in Ferm 5. When the glucose
427 concentration in the batch phase was increased from 2% to 3%, the isoprenol titer was
428 further improved, reaching a maximum of 6.84 g/L at 79 hours (yield of 0.084 g/g); no
429 significant accumulation of acetate was detected (see Ferm 6 in Figure 8) as was the case
430 for Ferm 5. The maximum OD_{600nm} was greater with 3% glucose in which additional
431 NH_4Cl was added to maintain a C/N = 10, reaching a value of 25 at 33 hours. This result
432 suggests that the conversion of glucose into isoprenol was further improved by increasing
433 biomass available during fed-batch phase. Based on these results, we used the strain with
434 the acetate-pathway genes deleted for further optimization of the isoprenol production
435 with 3% initial glucose.
436 **3.4.3. Use of a solvent overlay: two-phase cultivation**
437 As shown in Figure 8B, there was no significant increase in OD_{600nm} after 35 hours
438 regardless of acetate accumulation or higher glucose in the batch phase (Ferm 4-6). In
439 fact, most of the acetate accumulation in Ferm 4 was observed after 50 hours, suggesting
440 that acetate toxicity may not be the reason for the halted growth after 35 hours. Besides

441 acetate accumulation, there was an observed relationship between the time at which the
442 culture stopped growing and the time at which higher isoprenol titers were reached. As
443 shown in Figures 7 and 8, no significant increase in OD_{600nm} values was observed after
444 isoprenol titers reached more than 3 g/L, suggesting that high isoprenol concentration
445 might be a reason for the halted growth It is known that exposure to short-chain alcohols
446 can result in compromised cell membranes, causing uncontrolled transport of solutes,
447 leakage of important cofactors, and inactivation of membrane and cytosolic enzymes,
448 resulting in a decline in growth rate and cell viability (Huffer et al., 2011; Ingram, 1986).
449 In the case of *E. coli*, it has been reported that isoprenol can be toxic at concentrations as
450 low as 2.4 g/L (Foo et al., 2014). Two-phase cultivations, in which an organic solvent is
451 used to continuously extract a product *in situ*, can be used as a strategy to reduce the toxic
452 effects of the product and to increase its yield (Malinowski, 2001). In particular, oleyl
453 alcohol has been shown to be an effective solvent for the extraction of short-chain
454 alcohols in two-phase cultivations (Connor et al., 2010; Roffler et al., 1987).
455 Therefore, oleyl alcohol (20% v/v) was added to the bioreactor at the time of induction
456 and the cultivation was carried out as described in the previous section, except that
457 isoprenol was measured both in the aqueous and the organic phases. When the two-phase
458 cultivation with oleyl alcohol (Ferm 7) was used, significantly higher OD values were
459 achieved compared to those of the one-phase cultivation (Ferm 6; Figure 9A); moreover,
460 the OD_{600nm} from two-phase cultivation (Ferm 7) increased throughout cultivation and
461 reached a maximum value of 44.6 at 95 hours, which is a substantial improvement in
462 growth compared to Ferm 6. Accumulation of greater biomass during the two-phase
463 cultivation (Ferm 7) was confirmed by DCW measurements (see Supplementary Figure

S6A). Isoprenol production was also significantly higher when the two-phase cultivation strategy was used (Figure 9B), reaching a maximum titer of 10.8 g/L at 95 hr with a yield of 0.105 g/g glucose and a maximum productivity of 0.157 g L^{-1} hr^{-1}. Further analysis showed that the amount of isoprenol coming from the aqueous phase accounts for ca. 62% (6.7 g/L) of the total isoprenol produced and the amount of isoprenol coming from the oleyl alcohol phase accounts for ca. 38% (4.1 g/L) of the total isoprenol produced (Supplementary Figure S6C). It is noteworthy that the maximum aqueous-phase concentration of isoprenol for the two-phase cultivation was very similar to the maximum concentration reached in the fermentation without an overlay (see Figure 9B and Supplementary Figure S6D). This result shows that a continuous product extraction using an overlay can be an effective strategy for producing isoprenol at high titers and reducing its detrimental effect on growth by maintaining a low concentration of the toxic product in the producing culture.

Since the use of two-phase fermentations at larger scales could be challenging in terms of the cost and the downstream processing, production of isoprenol at high titers and at larger scales might require the development of strategies to alleviate the toxicity of isoprenol without the use of organic solvents. Improving *E. coli*'s tolerance to isoprenol by expressing efflux pumps or transporters (Foo et al., 2014) or by directed evolution is a promising strategy that could allow production at high titers without the need for two-phase fermentation, but further host engineering would be required for this goal.

4. Conclusion

The IPP-bypass pathway was optimized for production of isoprenol in *E. coli* by improving the biosynthesis of MVAP and its conversion to IP, a direct precursor of isoprenol. A series of metabolic engineering efforts improved the isoprenol production substantially, reaching 3.7 g/L (0.14 g isoprenol per g glucose) in batch fermentations using minimal medium. The use of fed-batch fermentation allowed production of isoprenol at 10.8 g/L, which is the highest reported titer for this compound. In addition to medium optimization and the elimination of acetate accumulation, production at high titers required the use of a two-phase cultivation process whereby isoprenol was partially removed from the aqueous phase into an organic overlay. The removal of isoprenol from the aqueous phase contributed to relieving its toxicity, resulting in considerably higher biomass levels in the cultivation with an organic overlay.

Acknowledgements

This work was part of the DOE Joint BioEnergy Institute (http://www.jbei.org) supported by the U.S. Department of Energy, Office of Science, Office of Biological and Environmental Research, through contract DE-AC02-05CH11231 between Lawrence Berkeley National Laboratory and the U.S. Department of Energy. The United States Government retains and the publisher, by accepting the article for publication, acknowledges that the United States Government retains a non-exclusive, paid-up, irrevocable, world-wide license to publish or reproduce the published form of this manuscript, or allow others to do so, for United States Government purposes.

References

Baidoo EEK, Wang G, Joshua CJ, Benites VT, Keasling JD. 2019. Liquid Chromatography and Mass Spectrometry Analysis of Isoprenoid Intermediates in Escherichia coli. In: . *Methods Mol. Biol.*, Vol. 1859, pp. 209–224.

Balan V. 2014. Current Challenges in Commercially Producing Biofuels from Lignocellulosic Biomass. *ISRN Biotechnol.* **2014**:1–31.

Baral NR, Kavvada O, Mendez-Perez D, Mukhopadhyay A, Lee TS, Simmons BA, Scown CD. 2019. Techno-economic analysis and life-cycle greenhouse gas mitigation cost of five routes to bio-jet fuel blendstocks. *Energy Environ. Sci.* **12**:807–824.

Basan M, Hui S, Okano H, Zhang Z, Shen Y, Williamson JR, Hwa T. 2015. Overflow metabolism in Escherichia coli results from efficient proteome allocation. *Nature* **528**:99–104.

Cheon S, Kim HM, Gustavsson M, Lee SY. 2016. Recent trends in metabolic engineering of microorganisms for the production of advanced biofuels. *Curr. Opin. Chem. Biol.* **35**:10–21.

Connor MR, Cann AF, Liao JC. 2010. 3-Methyl-1-butanol production in Escherichia coli: random mutagenesis and two-phase fermentation. *Appl. Microbiol. Biotechnol.* **86**:1155–1164.

Dugar D, Stephanopoulos G. 2011. Relative potential of biosynthetic pathways for biofuels and bio-based products. *Nat. Biotechnol.* **29**:1074–8.

Eiteman M a., Altman E. 2006. Overcoming acetate in Escherichia coli recombinant protein fermentations. *Trends Biotechnol.* **24**:530–536.

Foo JL, Jensen HM, Dahl RH, George K, Keasling JD, Lee TS, Leong S, Mukhopadhyay A. 2014. Improving Microbial Biogasoline Production in Escherichia coli Using Tolerance Engineering. *MBio* **5**:1–9.

George KW, Chen A, Jain A, Batth TS, Baidoo EEK, Wang G, Adams PD, Petzold CJ, Keasling JD, Lee TS. 2014. Correlation analysis of targeted proteins and metabolites to assess and engineer microbial isopentenol production. *Biotechnol. Bioeng.* **111**:1648–1658.

George KW, Thompson MG, Kang A, Baidoo E, Wang G, Chan LJG, Adams PD, Petzold CJ, Keasling JD, Soon Lee T. 2015. Metabolic engineering for the high-yield production of isoprenoid-based C5 alcohols in E. coli. *Sci. Rep.* **5**:11128.

Hollinshead W, He L, Tang YJ. 2014. Biofuel production: an odyssey from metabolic engineering to fermentation scale-up. *Front. Microbiol.* **5**:344.

Huffer S, Clark ME, Ning JC, Blanch HW, Clark DS. 2011. Role of Alcohols in Growth, Lipid Composition, and Membrane Fluidity of Yeasts, Bacteria, and Archaea. *Appl. Environ. Microbiol.* **77**:6400–6408.

Hugo WB, Lund BM. 1968. The effect of supplementationof the growth medium with yeast extract, on dehydrogenase activity of Escherichia coli. *J . appl. Bact* **21**:249–256.

Ingram LO. 1986. Microbial tolerance to alcohols: role of the cell membrane. *Trends Biotechnol.* **4**:40–44.

Kang A, George KW, Wang G, Baidoo E, Keasling JD, Lee TS. 2016. Isopentenyl diphosphate (IPP)-bypass mevalonate pathways for isopentenol production. *Metab. Eng.* **34**:25–35.

Kang A, Meadows CW, Canu N, Keasling JD, Lee TS. 2017. High-throughput enzyme screening platform for the IPP-bypass mevalonate pathway for isopentenol production. *Metab. Eng.* **41**:125–134.

Korz DJ, Rinas U, Hellmuth K, Sanders E a., Deckwer WD. 1995. Simple fed-batch technique for high cell density cultivation of Escherichia coli. *J. Biotechnol.* **39**:59–65.

Li M, Nian R, Xian M, Zhang H. 2018. Metabolic engineering for the production of isoprene and isopentenol by Escherichia coli. *Appl. Microbiol. Biotechnol.* **102**:7725–7738.

Liao JC, Mi L, Pontrelli S, Luo S. 2016. Fuelling the future: microbial engineering for the production of sustainable biofuels. *Nat. Rev. Microbiol.* **14**:288–304.

Liu H, Wang Y, Tang Q, Kong W, Chung W-J, Lu T. 2014. MEP pathway-mediated isopentenol production in metabolically engineered Escherichia coli. *Microb. Cell Fact.* **13**:135.

Ma SM, Garcia DE, Redding-Johanson AM, Friedland GD, Chan R, Batth TS, Haliburton JR, Chivian D, Keasling JD, Petzold CJ, Soon Lee T, Chhabra SR. 2011. Optimization of a heterologous mevalonate pathway through the use of variant HMG-CoA reductases. *Metab. Eng.* **13**:588–597.

Mack JH, Rapp VH, Broeckelmann M, Lee TS, Dibble RW. 2014. Investigation of biofuels from microorganism metabolism for use as anti-knock additives. *Fuel* **117**:939–943.

Malinowski JJ. 2001. Two-phase partitioning bioreactors in fermentation technology. *Biotechnol. Adv.* **19**:525–538.

Meadows CW, Kang A, Lee TS. 2018. Metabolic Engineering for Advanced Biofuels Production and Recent Advances Toward Commercialization. *Biotechnol. J.* **13**:1600433.

De Mey M, De Maeseneire S, Soetaert W, Vandamme E. 2007. Minimizing acetate formation in E. coli fermentations. *J. Ind. Microbiol. Biotechnol.* **34**:689–700.

Rabinovitch-Deere C a, Oliver JWK, Rodriguez GM, Atsumi S. 2013. Synthetic biology and metabolic engineering approaches to produce biofuels. *Chem. Rev.* **113**:4611–32.

Roffler SR, Blanch HW, Wilke CR. 1987. In-situ recovery of butanol during fermentation Part 1: Batch extractive fermentation. *Bioprocess Eng.* **2**:1–12.

Singh V, Haque S, Niwas R, Srivastava A, Pasupuleti M, Tripathi CKM. 2017. Strategies for fermentation medium optimization: An in-depth review. *Front. Microbiol.* **7**.

Szenk M, Dill KA, de Graff AMR. 2017. Why Do Fast-Growing Bacteria Enter Overflow Metabolism? Testing the Membrane Real Estate Hypothesis. *Cell Syst.* **5**:95–104.

Tian T, Kang JW, Kang A, Lee TS. 2019. Redirecting Metabolic Flux via Combinatorial Multiplex CRISPRi-Mediated Repression for Isopentenol Production in Escherichia coli. *ACS Synth. Biol.* **8**:391–402.

Volkmer B, Heinemann M. 2011. Condition-Dependent Cell Volume and Concentration of Escherichia coli to Facilitate Data Conversion for Systems Biology Modeling. Ed. Jörg Langowski. *PLoS One* **6**:e23126.

Wehrs M, Tanjore D, Eng T, Lievense J, Pray TR, Mukhopadhyay A. 2019. Engineering Robust Production Microbes for Large-Scale Cultivation. *Trends Microbiol.*

Wolfe AJ. 2005. The Acetate Switch. *Microbiol. Mol. Biol. Rev.* **69**:12–50.

Ye L, Lv X, Yu H. 2016. Engineering microbes for isoprene production. *Metab. Eng.* **38**:125–138.

Zada B, Wang C, Park J-B, Jeong S-H, Park J-E, Singh HB, Kim S-W. 2018. Metabolic engineering of Escherichia coli for production of mixed isoprenoid alcohols and their derivatives. *Biotechnol. Biofuels* **11**:210.

607 Zheng Y, Liu Q, Li L, Qin W, Yang J, Zhang H, Jiang X, Cheng T, Liu W, Xu X, Xian
608 M. 2013. Metabolic engineering of Escherichia coli for high-specificity production
609 of isoprenol and prenol as next generation of biofuels. *Biotechnol. Biofuels* **6**:57.

610

611 **Table 1. Strains and plasmids used in this work**

Strain	Description	Reference
DH1	Wild type DH1	
AK01	DH1 with plasmids JBEI-9310 + JBEI-9314	(Kang et al., 2016)
AK02	DH1 with plasmids JBEI-2703 + JBEI-12064	This work
AK03	DH1 with plasmids JBEI-17856 and JBEI-12064	This work
AK04	DH1 with plasmids JBEI-3093 and JBEI-12064	This work
AK05	DH1 with plasmids JBEI-3092 and JBEI-12064	This work
AK06	DH1 with plasmids JBEI-17835 and JBEI-12064	This work
AK07	DH1 with plasmids JBEI-3100 and JBEI-12064	This work
AK08	DH1 with plasmids JBEI-17837 and JBEI-12064	This work
AK09	DH1 with plasmids JBEI-17081 and JBEI-12064	This work
AK10	DH1 with plasmids JBEI-3100 and JBEI-17847	This work
AK11	DH1 with plasmids JBEI-3100 and JBEI-17864	This work
AK12	DH1 with plasmids JBEI-3100 and JBEI-17865	This work
AK13	DH1 with plasmids JBEI-17081 and JBEI-17847	This work
AK14	DH1 with plasmids JBEI-3100 and JBEI-17866	This work
AK15	DH1 with plasmids JBEI-3100 and JBEI-17862	This work
AK16	DH1 with plasmids JBEI-3100 and JBEI-17861	This work
AK18	DH1 with plasmids JBEI-3100 and JBEI-17853	This work
AK19	DH1 with plasmids JBEI-3100 and JBEI-17852	This work
AK20	DH1 with plasmids JBEI-3100 and JBEI-17857	This work
AK21	DH1 with plasmids JBEI-3100 and JBEI-17839	This work
AK22	DH1 with plasmids JBEI-3100 and JBEI-17841	This work
AK23	DH1 with plasmids JBEI-3100 and JBEI-17840	This work
AK24	DH1 with plasmids JBEI-17081 and JBEI-17846	This work
AK25	DH1 with plasmids JBEI-17081 and JBEI-17845	This work
AK26	DH1 with plasmids JBEI-17081 and JBEI-17844	This work
AK27	DH1 with plasmids JBEI-17081 and JBEI-17839	This work
AK28	DH1 with plasmids JBEI-17081 and JBEI-17841	This work
AK29	DH1 with plasmids JBEI-17081 and JBEI-17840	This work
DH1-KO	DH1 *Δpta-ackA ΔpoxB*	(Tian et al., 2019)
AK30	DH1-KO with plasmids JBEI-17081 and JBEI-17844	This work

612

Plasmid	Description	Reference
JBEI-9310	pA5c- AtoB-HMGS_Sc_o-HMGR_Sc_o-MK_co	(Kang et al., 2016)
JBEI-9314	pTrc99a-PMDsc	(Kang et al., 2016)
JBEI-2703	pA5c-AtoB-HMGS_Sc_o-HMGR_Sc_o	(Ma et al., 2011)
JBEI-17856	pA5c-AtoB-HMGS_Sc_o-HMGR_Pm	(Ma et al., 2011)
JBEI-3093	pA5c-AtoB-HMGS_Sc_o-HMGR_Da	(Ma et al., 2011)

JBEI-3092	pA5c-AtoB-HMGS_Sc_o-HMGR_Bp	(Ma et al., 2011)
JBEI-17835	pA5c-AtoB-HMGS_Sc_co-HMGR_Bp	This work
JBEI-3100	pA5c-AtoB-HMGS_Sc_co-HMGR_Sc_co	(Ma et al., 2011)
JBEI-17837	pA5c-AtoB-HMGS_Sc_co-HMGR_Sa	This work
JBEI-17081	pA5c-AtoB-HMGS_Sa-HMGR_Sa	(Ma et al., 2011)
JBEI-12064	pTrc99a-PMDsc-MK_co	(Kang et al., 2016)
JBEI-17847	pTrc99a-PMDsc-MK_Mm	This work
JBEI-17864	pTrc99a-PMDsc-MK_Sa	This work
JBEI-17865	pTrc99a-PMDsc-MK_Sn	This work
JBEI-17866	pTrc99a-PMDsc-MK_co-HMGR_Bp	This work
JBEI-17862	pTrc99a-PMDsc-MK_co-HMGR_Da	This work
JBEI-17861	pTrc99a-PMDsc-MK_co-HMGR_Pm	This work
JBEI-17853	pTrc99a-PMDsc-MK_co-HMGR_Sc_o	This work
JBEI-17852	pTrc99a-PMDsc-MK_co-HMGR_Sc_co	This work
JBEI-17857	pTrc99a-PMDsc-MK_co-HMGR_Sa	This work
JBEI-17844	pTrc99a-PMDsc_HKQ-MKmm	This work
JBEI-17846	pTrc99a-PMDsc_R74G-MKmm	This work
JBEI-17845	pTrc99a-PMDsc_R74H-MKmm	This work
JBEI-17840	pTrc99a-PMDsc_HKQ-MK_Sc_co	This work
JBEI-17839	pTrc99a-PMDsc_R74G-MK_Sc_co	This work
JBEI-17841	pTrc99a-PMDsc_R74H-MK_Sc_co	This work

613

614

FIGURE LEGENDS

Figure 1. Isoprenol production pathway and plasmids for heterologous pathway expression (A) Pathway reactions and relevant enzymes for isoprenol production. Heterologous enzymes targeted for engineering are highlighted in filled dark arrows. (B-D) configuration of two plasmids used in this study. (B) Configuration used only in strain AK01. (C) Format used for MK variants, HMGS-HMGR variants, and PMD variants. (D) Format used for the expression of additional HMGR.

Figure 2. Optimization of intermediates for MVAP biosynthesis. (A) Isoprenol titer with MK expressed from a medium-copy plasmid (p15A origin) or high-copy plasmid (ColE1 origin); (B) Production with HMGS and HMGR from different sources; (C) Isoprenol production with MK from various sources; (D) Expression of an additional copy of HMGR. Error bars represent one standard deviation from three biological replicates. Cultures were grown in test tubes with EZ-Rich medium at 30°C, induction at OD_{600nm} = 0.4-0.6 with 0.5 mM IPTG, and isoprenol production was measured at 48 hr. Sc_o: *S. cerevisiae* wild type, Sc_co: *S. cerevisiae* codon optimized, Sa: *S. aureus*, Bp: *Bordetella petrii*, Da: *Delftia acidovorans*, Pm: *Pseudomonas mevalonii*, Mm: *M. masei*, Sn: *Streptococcus pneumoniae*, MK: mevalonate kinase, HMGS=HMG-CoA synthase, HMGR= HMG-CoA reductase

Figure 3. Comparison of strains containing wild-type PMD (strain AK07) and the R74G PMD mutant (strain AK21). (A) Isoprenol production and growth; (B) Mevalonate (MVA) and mevalonate phosphate (MVAP) levels. Error bars represent one standard

deviation from three biological replicates of EZ-Rich medium (50 mL in 250-mL flasks) supplemented with 1% glucose at 30°C.

Figure 4. Effect of PMD mutants and HMGS-HMGR-MK systems on isoprenol production. (A) Production in EZ-Rich medium; (B) Production in minimal medium. PDM with the single mutations R74G or R74H, or with triple mutation R74H, R147K, and M212Q (HKQ) were tested with different HMGS, HMGR, and MK. Figure shows the average of three biological replicates of cultures grown at 30°C. EZ Rich medium was supplemented with 1% glucose and isoprenol production was measured at 48 hr. Minimal medium was supplemented with 2% glucose and isoprenol production was measured at 63 hr. Sc_co = *S. cerevisiae,* codon-optimized; Sa = *S. aureus*; Mm = *M. mazei.*

Figure 5. Data from strain AK26 grown on minimal medium supplemented with 1% and 2% glucose. (A) Growth; (B) glucose concentration in the medium; (C) isoprenol production. Cultures were grown in flasks at 30°C and error bars represent one standard deviation from three biological replicates.

Figure 6. Comparison of the optimized strains (AK21, AK26, and AK27) in minimal medium supplemented with 3% glucose at different time points. (A) Isoprenol production; (B) Acetate accumulation; (C) Glucose consumption; (D) Ethanol accumulation. Cultures were grown in test tubes at 30°C and induced at OD_{600nm} 0.4-0.6 with 0.5 mM IPTG.

Figure 7. Media and feeding optimization. (A) Isoprenol titer; (B) optical density (OD_{600nm}). Fermentations were run at 30°C with 2% glucose in the batch medium using strain AK26. Ferm 1: batch medium with C/N=18 and constant feeding, feed started at 54 hours; Ferm 2: batch medium with C/N=10 and constant feeding, feed started at 31 hours; Ferm 3: batch medium with C/N=10 and exponential feeding, feed started at 31 hours; Ferm 4: batch medium with C/N=10, 10 g/L yeast extract and exponential feeding, feed started at 23 hours.

Figure 8. Elimination of acetate production. (A) acetate accumulation; (B) optical density (OD_{600nm}); (C) isoprenol titer; (D) glucose consumption. Fermentations were run at 30°C with 10 g/L yeast extract in the batch medium and exponential feeding. Ferm 4: DH1 strain, batch medium with 2% glucose (strain AK26), feed started at 23 hours; Ferm 5: DH1 Δ*poxB* Δ*ackA* Δ*pta* strain, batch medium with 2% glucose (strain AK30), feed started at 23 hours; Ferm 6: DH1 Δ*poxB* Δ*ackA* Δ*pta* strain, batch medium with 3% glucose (strain AK30), feed started at 25 hours.

Figure 9. Two-phase fermentation. (A) Optical density (OD_{600nm}); (B) isoprenol titer. Fermentations using the DH1 Δ*poxB* Δ*ackA* Δ*pta* strain (AK30), run at 30°C with 3% glucose and 10 g/L yeast extract in the batch medium, exponential feeding. Ferm 6: without overlay; Ferm 7: with 20% (v/v) oleyl alcohol overlay. For both Ferm 6 and 7, feed started at 25 hours.

Figure 1


(A)
Glycolysis
PoxB
Acetate
Pyruvate
AckA
Acetyl-P
Pta
Acetyl-CoA
AtoB
HMGS
HMG
HMGR
MVA
MK
MVAP
PMD
IP
Isoprenol
TCA cycle

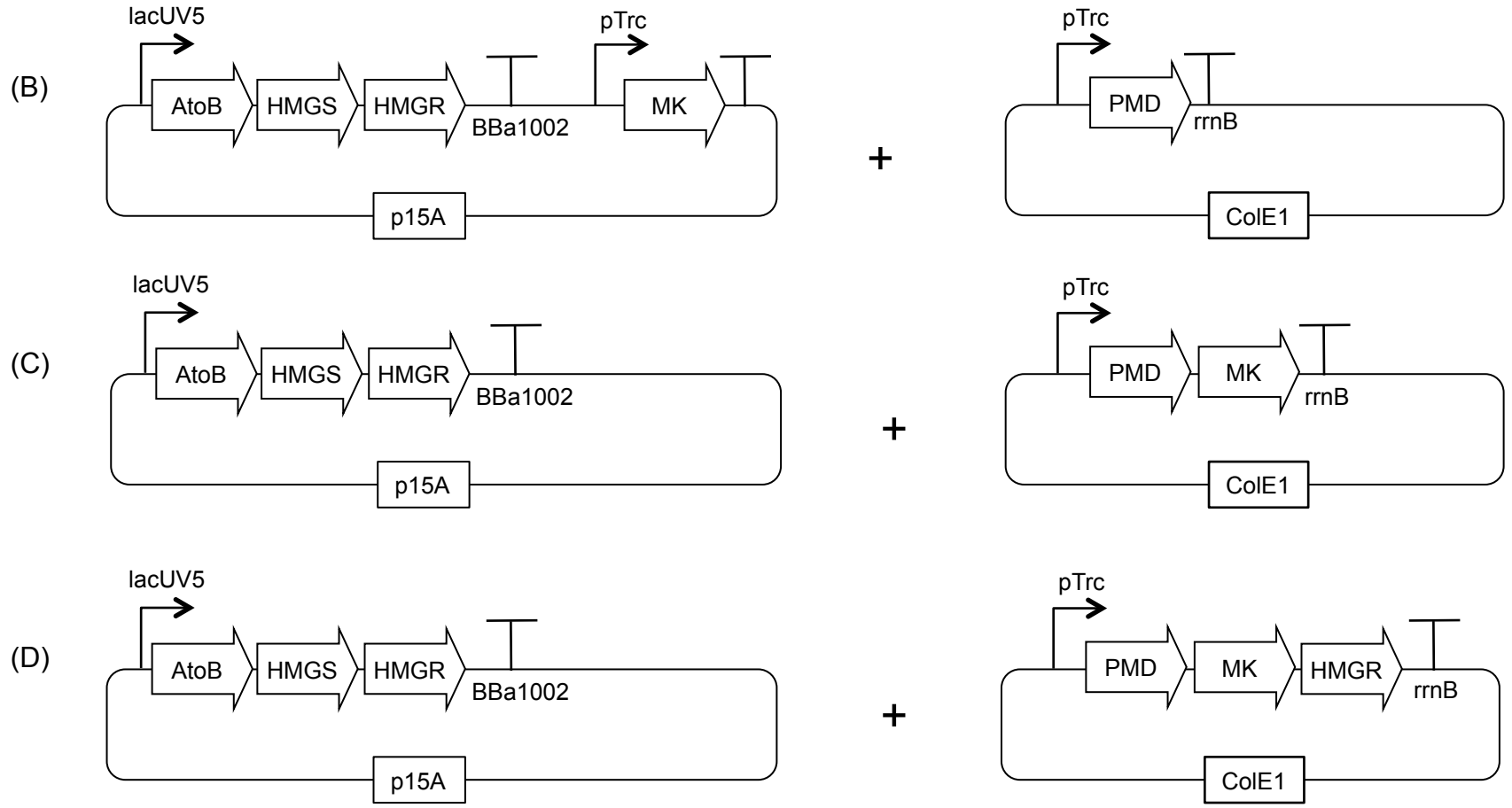
(B)
lacUV5
AtoB
HMGS
HMGR
BBa1002
pTrc
MK
p15A
+
pTrc
PMD
rrnB
ColE1
(C)
lacUV5
AtoB
HMGS
HMGR
BBa1002
p15A
+
pTrc
PMD
MK
rrnB
ColE1
(D)
lacUV5
AtoB
HMGS
HMGR
BBa1002
p15A
+
pTrc
PMD
MK
HMGR
rrnB
ColE1

Figure 2

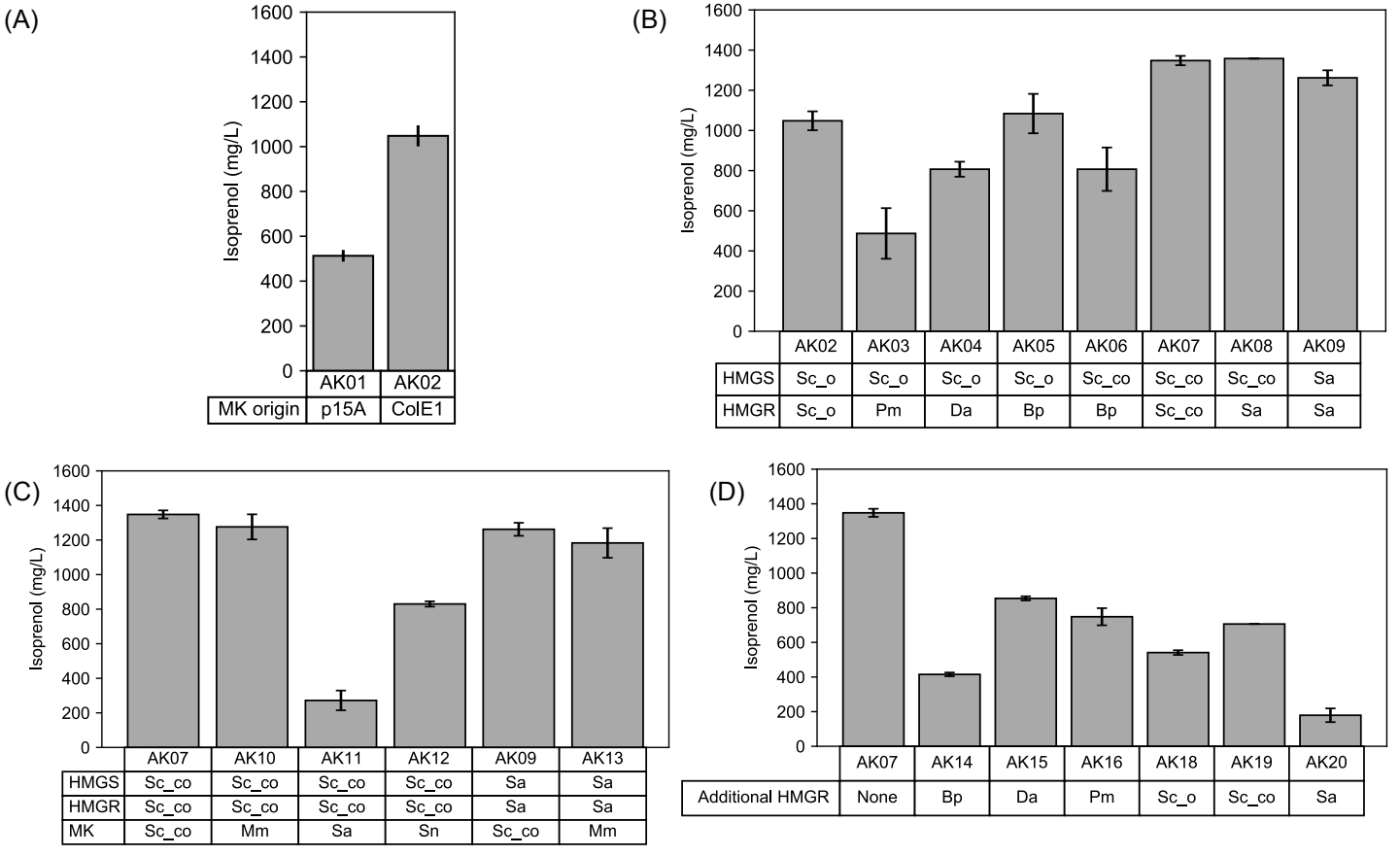
(A)
Isoprenol (mg/L)
1600
1400
1200
1000
800
600
400
200
0
AK01 AK02
MK origin p15A ColE1
(B)
Isoprenol (mg/L)
AK02 AK03 AK04 AK05 AK06 AK07 AK08 AK09
HMGS Sc_o Sc_o Sc_o Sc_o Sc_co Sc_co Sc_co Sa
HMGR Sc_o Pm Da Bp Bp Sc_co Sa Sa
(C)
Isoprenol (mg/L)
AK07 AK10 AK11 AK12 AK09 AK13
HMGS Sc_co Sc_co Sc_co Sc_co Sa Sa
HMGR Sc_co Sc_co Sc_co Sc_co Sa Sa
MK Sc_co Mm Sa Sn Sc_co Mm
(D)
Isoprenol (mg/L)
AK07 AK14 AK15 AK16 AK18 AK19 AK20
Additional HMGR None Bp Da Pm Sc_o Sc_co Sa

Figure 3

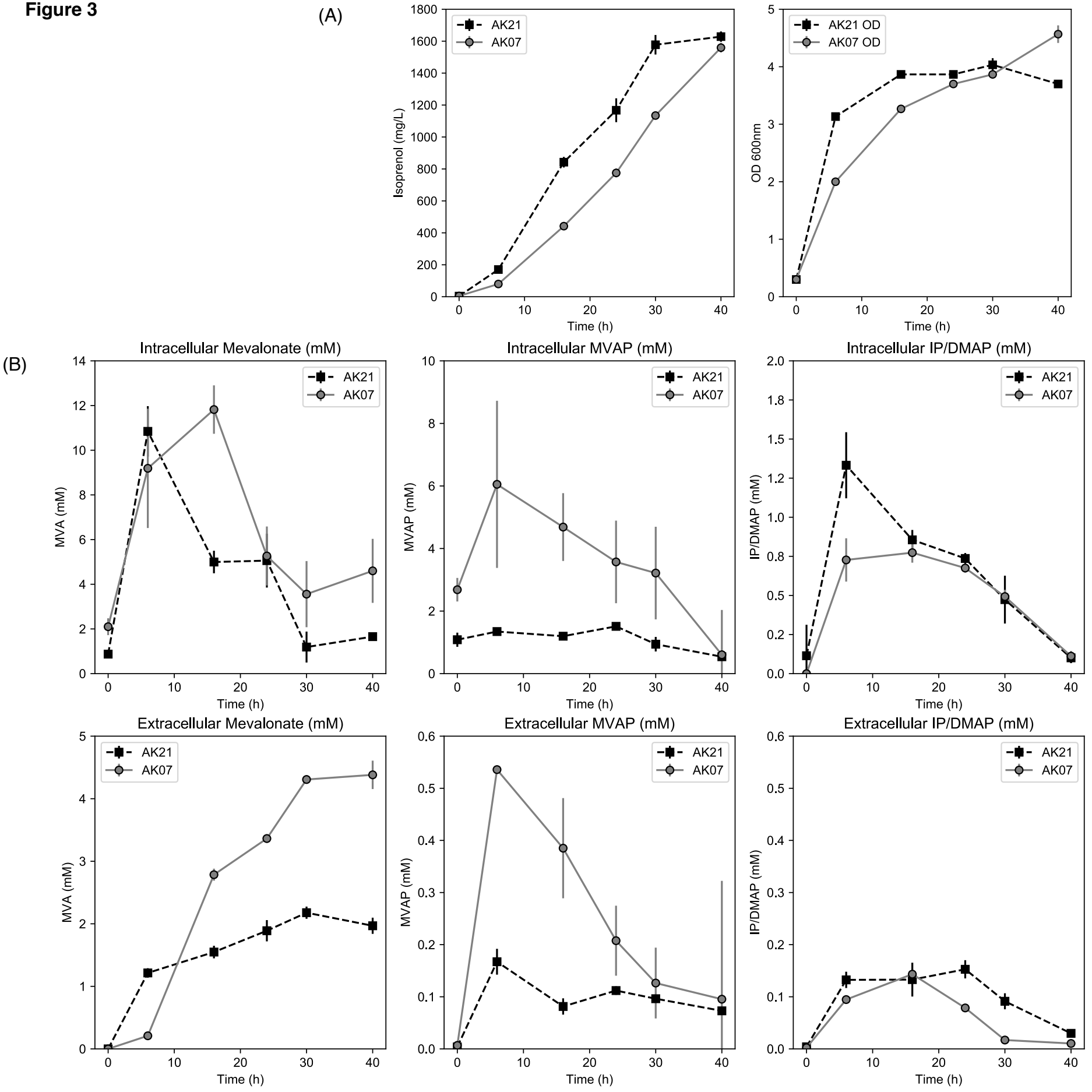
(A)
AK21
AK07
Isoprenol (mg/L)
Time (h)
AK21 OD
AK07 OD
OD 600nm
(B)
Intracellular Mevalonate (mM)
MVA (mM)
Intracellular MVAP (mM)
MVAP (mM)
Intracellular IP/DMAP (mM)
IP/DMAP (mM)
Extracellular Mevalonate (mM)
Extracellular MVAP (mM)
Extracellular IP/DMAP (mM)

Figure 4.

(A)

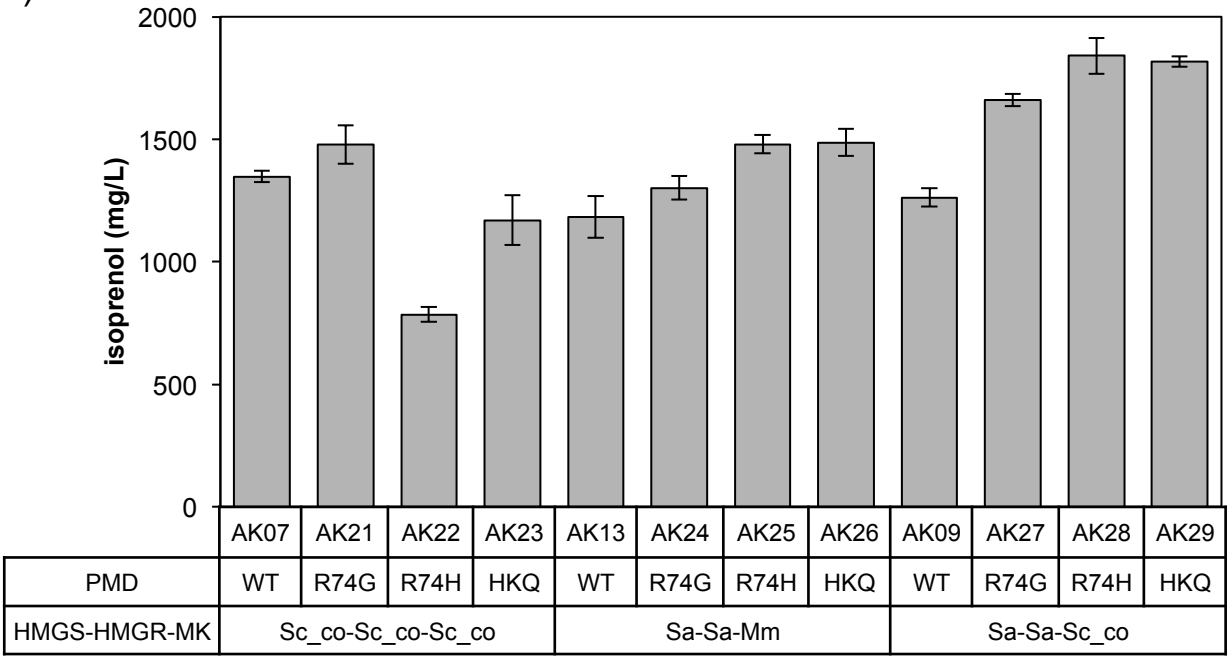
2000
1500
1000
500
0
isoprenol (mg/L)
AK07 AK21 AK22 AK23 AK13 AK24 AK25 AK26 AK09 AK27 AK28 AK29
PMD WT R74G R74H HKQ WT R74G R74H HKQ WT R74G R74H HKQ
HMGS-HMGR-MK Sc_co-Sc_co-Sc_co Sa-Sa-Mm Sa-Sa-Sc_co

(B)

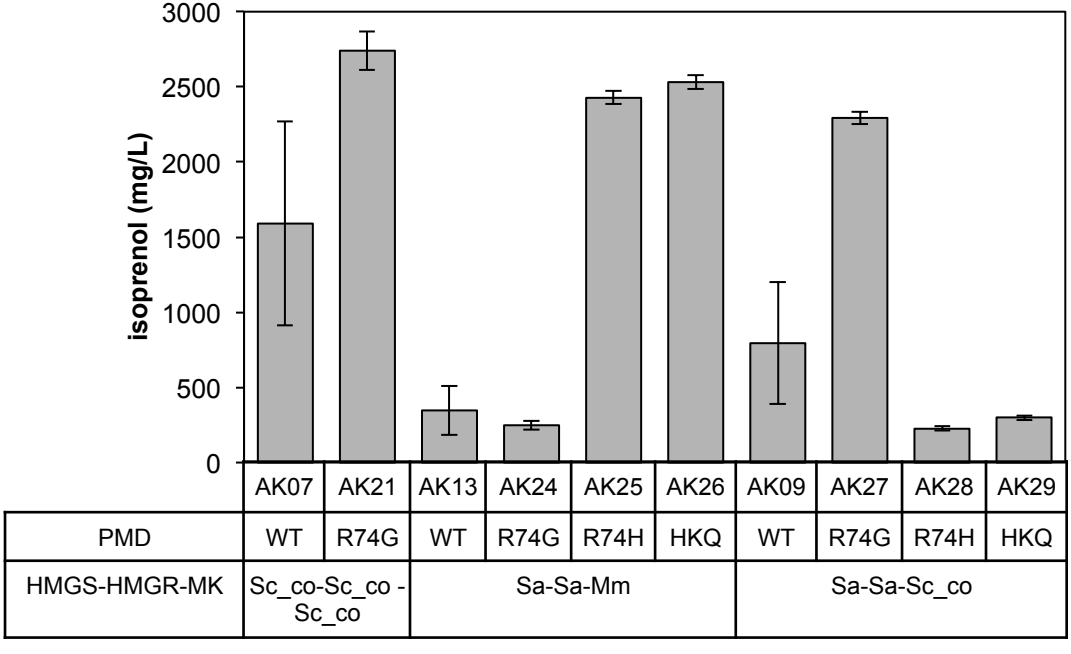
3000
2500
2000
1500
1000
500
0
isoprenol (mg/L)
AK07 AK21 AK13 AK24 AK25 AK26 AK09 AK27 AK28 AK29
PMD WT R74G WT R74G R74H HKQ WT R74G R74H HKQ
HMGS-HMGR-MK Sc_co-Sc_co - Sc_co Sa-Sa-Mm Sa-Sa-Sc_co

Figure 5

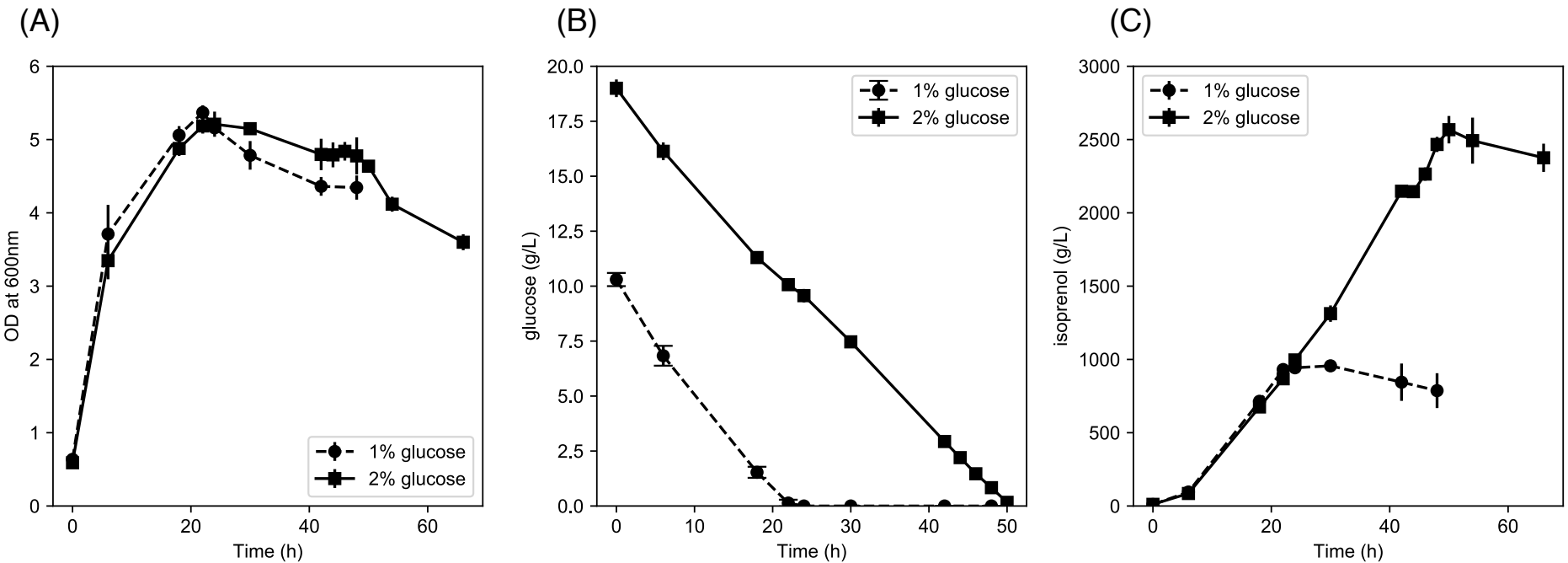
(A)
OD at 600nm
Time (h)
1% glucose
2% glucose
(B)
glucose (g/L)
Time (h)
1% glucose
2% glucose
(C)
isoprenol (g/L)
Time (h)
1% glucose
2% glucose

Figure 6

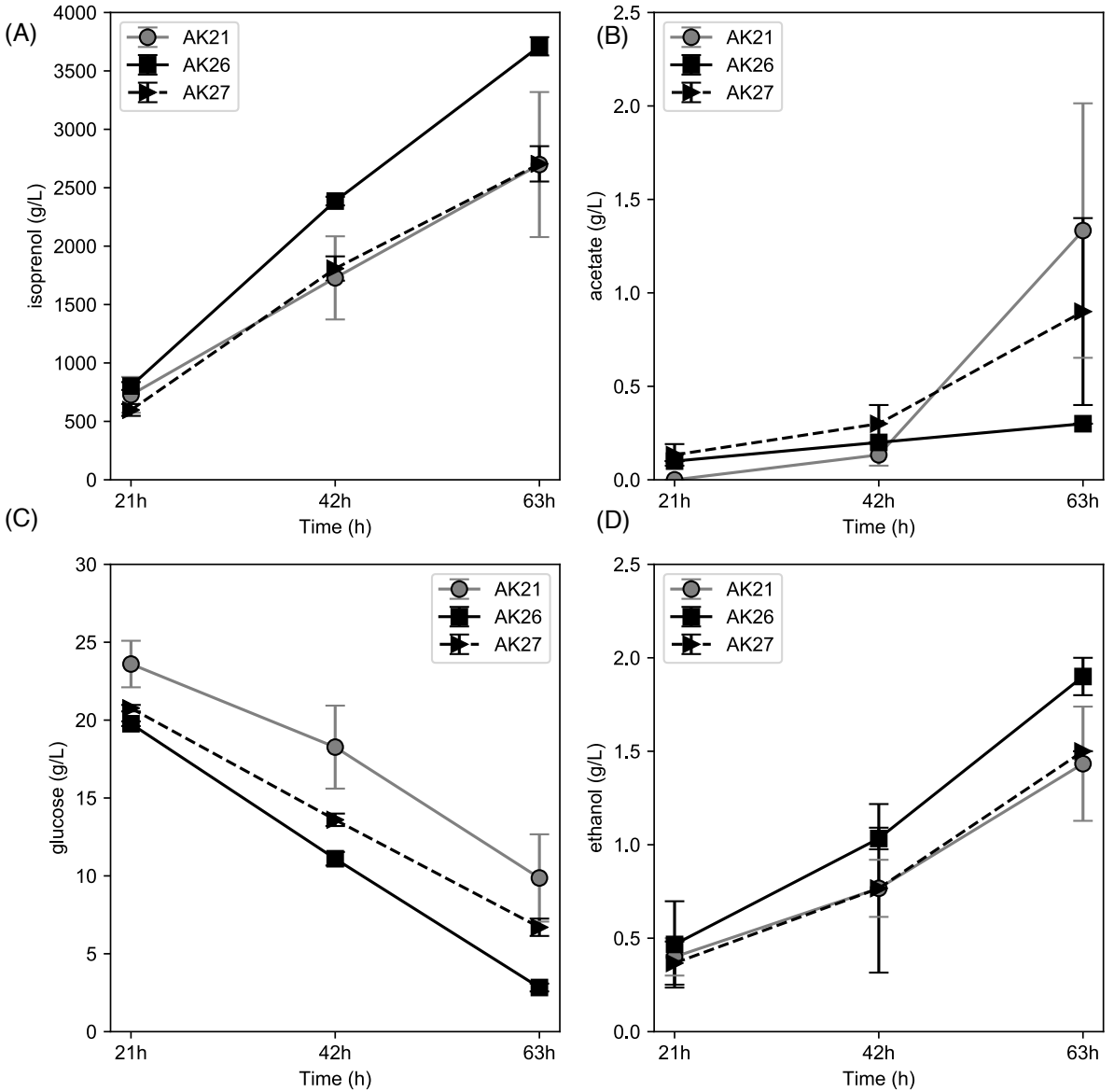
(A)
AK21
AK26
AK27
isoprenol (g/L)
4000
3500
3000
2500
2000
1500
1000
500
0
21h
42h
63h
Time (h)
(B)
AK21
AK26
AK27
acetate (g/L)
2.5
2.0
1.5
1.0
0.5
0.0
21h
42h
63h
Time (h)
(C)
AK21
AK26
AK27
glucose (g/L)
30
25
20
15
10
5
0
21h
42h
63h
Time (h)
(D)
AK21
AK26
AK27
ethanol (g/L)
2.5
2.0
1.5
1.0
0.5
0.0
21h
42h
63h
Time (h)

Figure 7

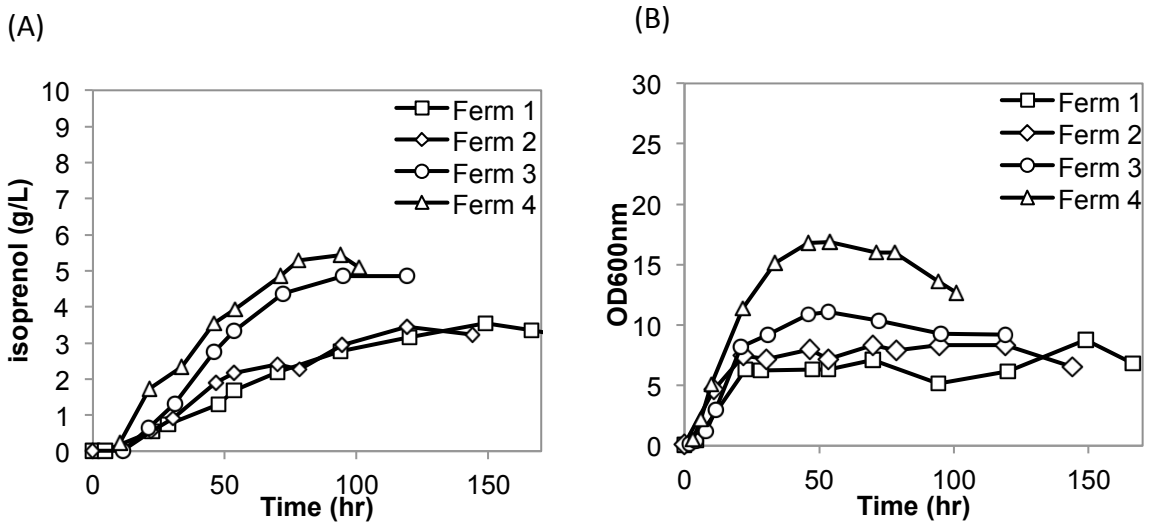
(A)
isoprenol (g/L)
Time (hr)
Ferm 1
Ferm 2
Ferm 3
Ferm 4
(B)
OD600nm
Time (hr)
Ferm 1
Ferm 2
Ferm 3
Ferm 4

Figure 8

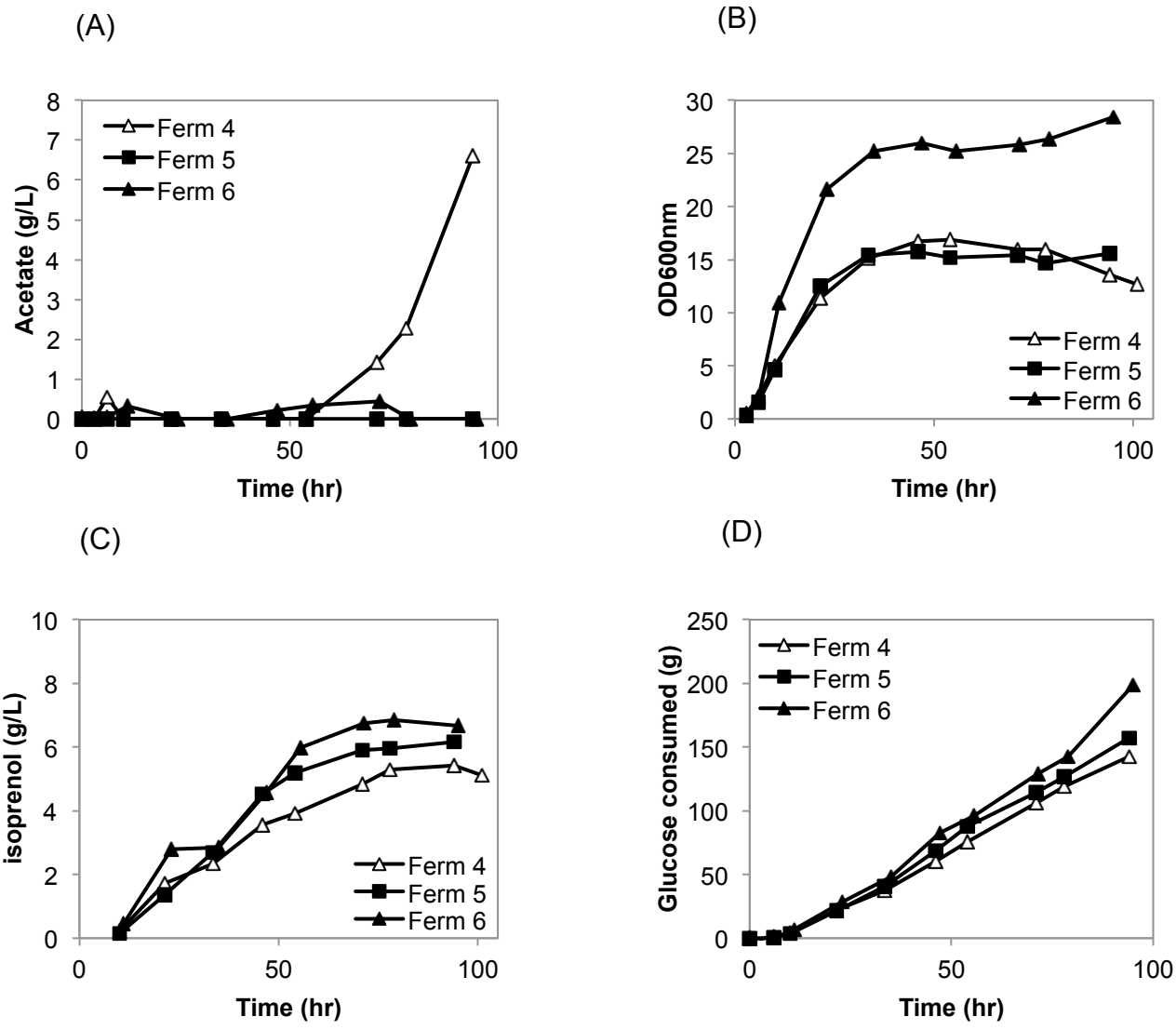
(A)
Acetate (g/L)
Time (hr)
Ferm 4
Ferm 5
Ferm 6
(B)
OD600nm
Time (hr)
Ferm 4
Ferm 5
Ferm 6
(C)
isoprenol (g/L)
Time (hr)
Ferm 4
Ferm 5
Ferm 6
(D)
Glucose consumed (g)
Time (hr)
Ferm 4
Ferm 5
Ferm 6

Figure 9

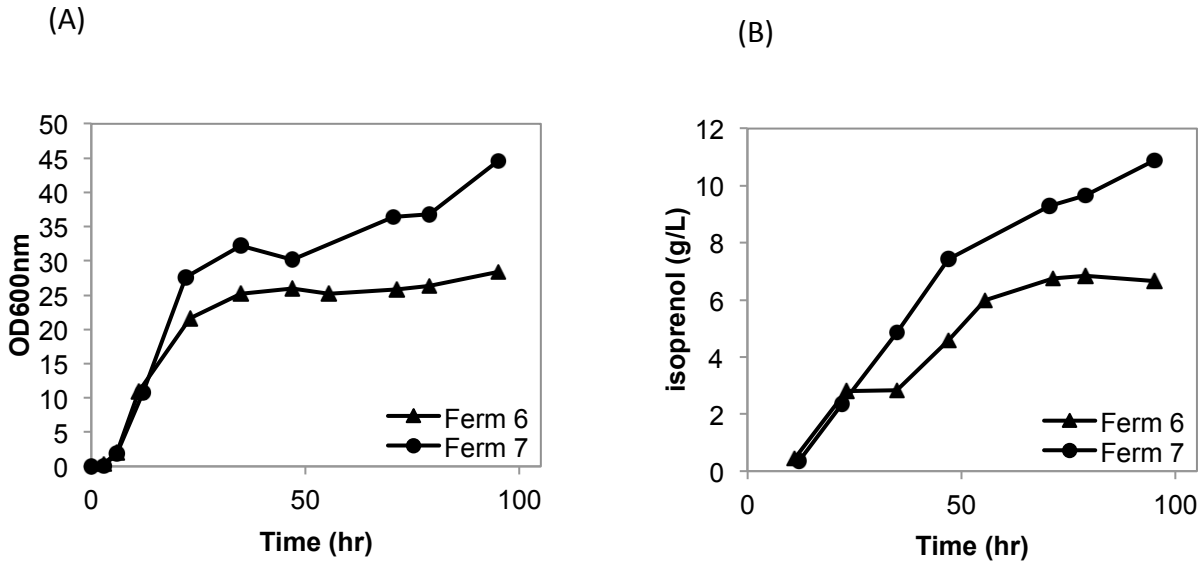
(A)
OD600nm
Time (hr)
Ferm 6
Ferm 7
(B)
isoprenol (g/L)
Time (hr)
Ferm 6
Ferm 7

Supplementary Figure S1. Analysis of additional HMGR expression on (A) growth by OD_{600nm}, (B) isoprenol production, and (C) intracellular and extracellular intermediate concentrations

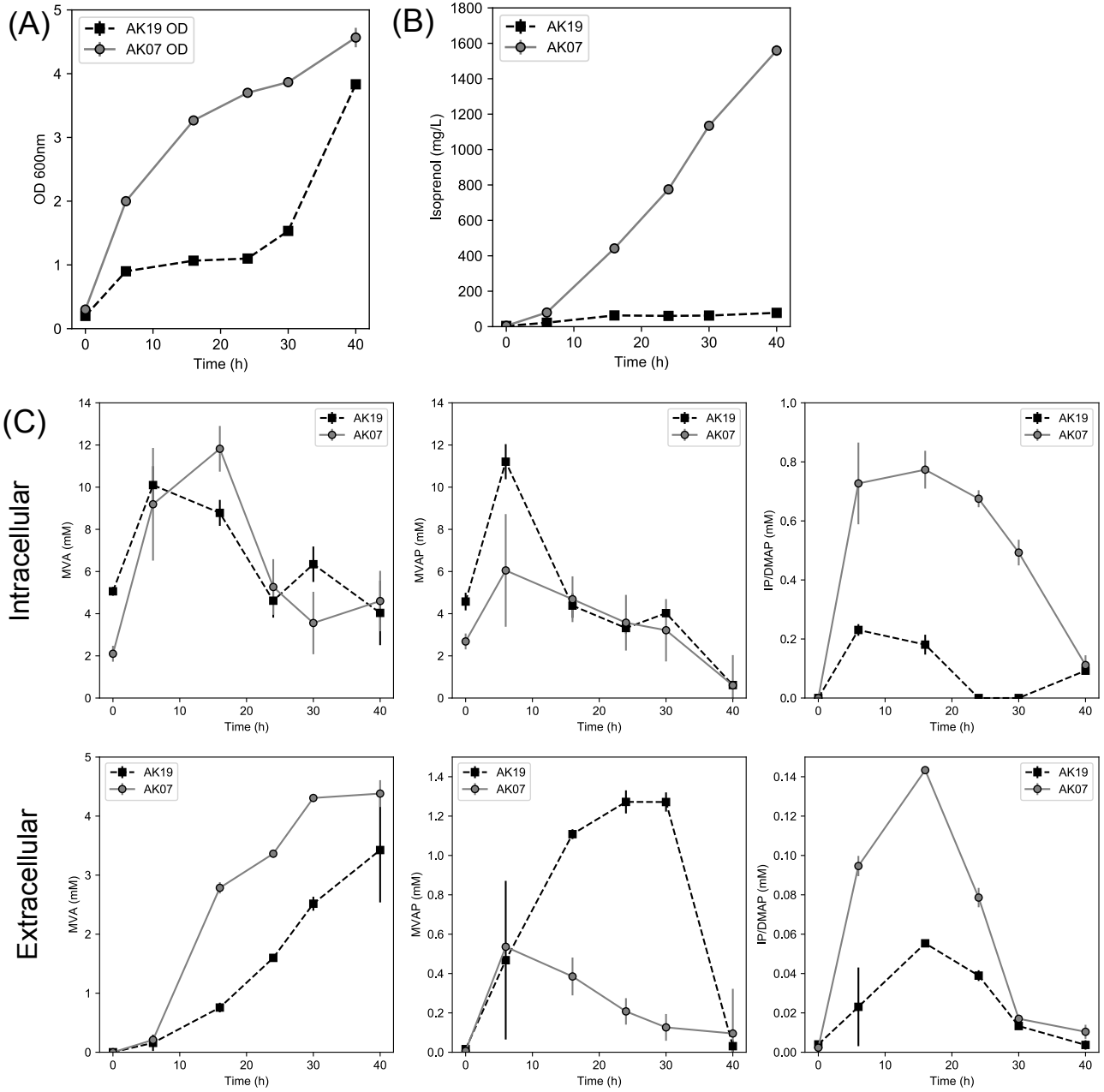

Supplementary Figure S2. Comparison of strains containing the wild type PMD (strain AK07) and the PMD with the R74G mutation (strain AK21). (A) Glucose remaining in the medium, (B) Acetate

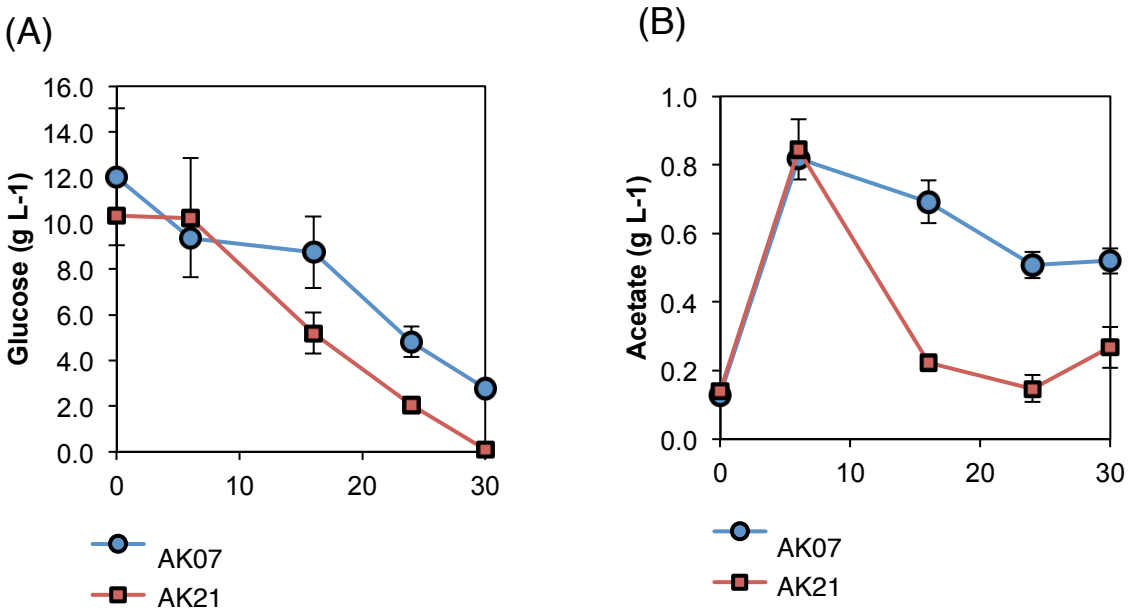

Supplementary Figure S3. Production in minimal medium supplemented with 1% glucose. Production was measured at 24 hours.

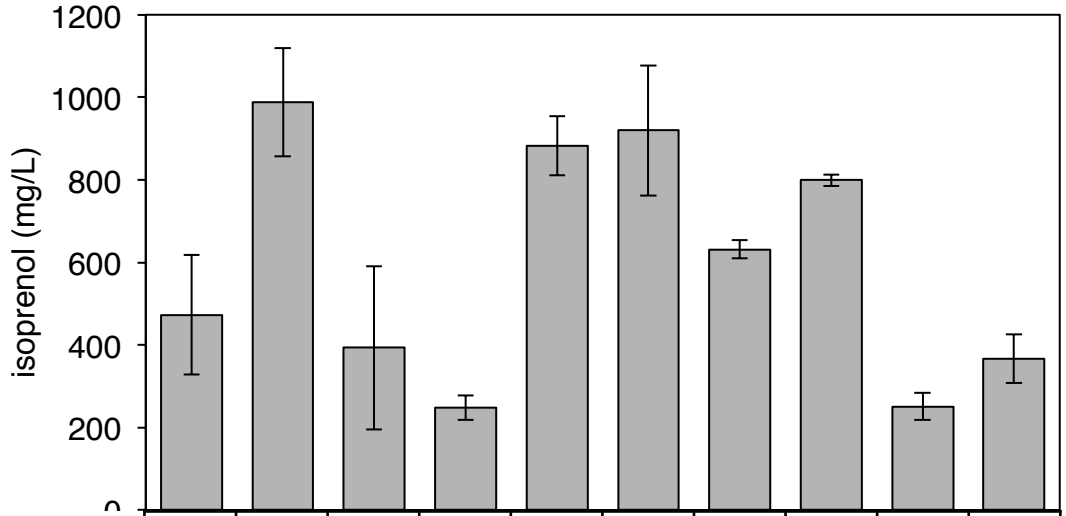

	AK07	AK21	AK13	AK24	AK25	AK26	AK09	AK27	AK28	AK29
PMD	WT	R74G	WT	R74G	R74H	HKQ	WT	R74G	R74H	HKQ
HMGS-HMGR-MK	Sc_co-Sc_co - Sc_co		Sa-Sa-Mm				Sa-Sa-Sc_co			

Supplementary Figure S4. Comparison of strain AK26 grown on minimal medium supplemented with 1% and 2% glucose. (A) Acetate accumulation; (B) Ethanol accumulation

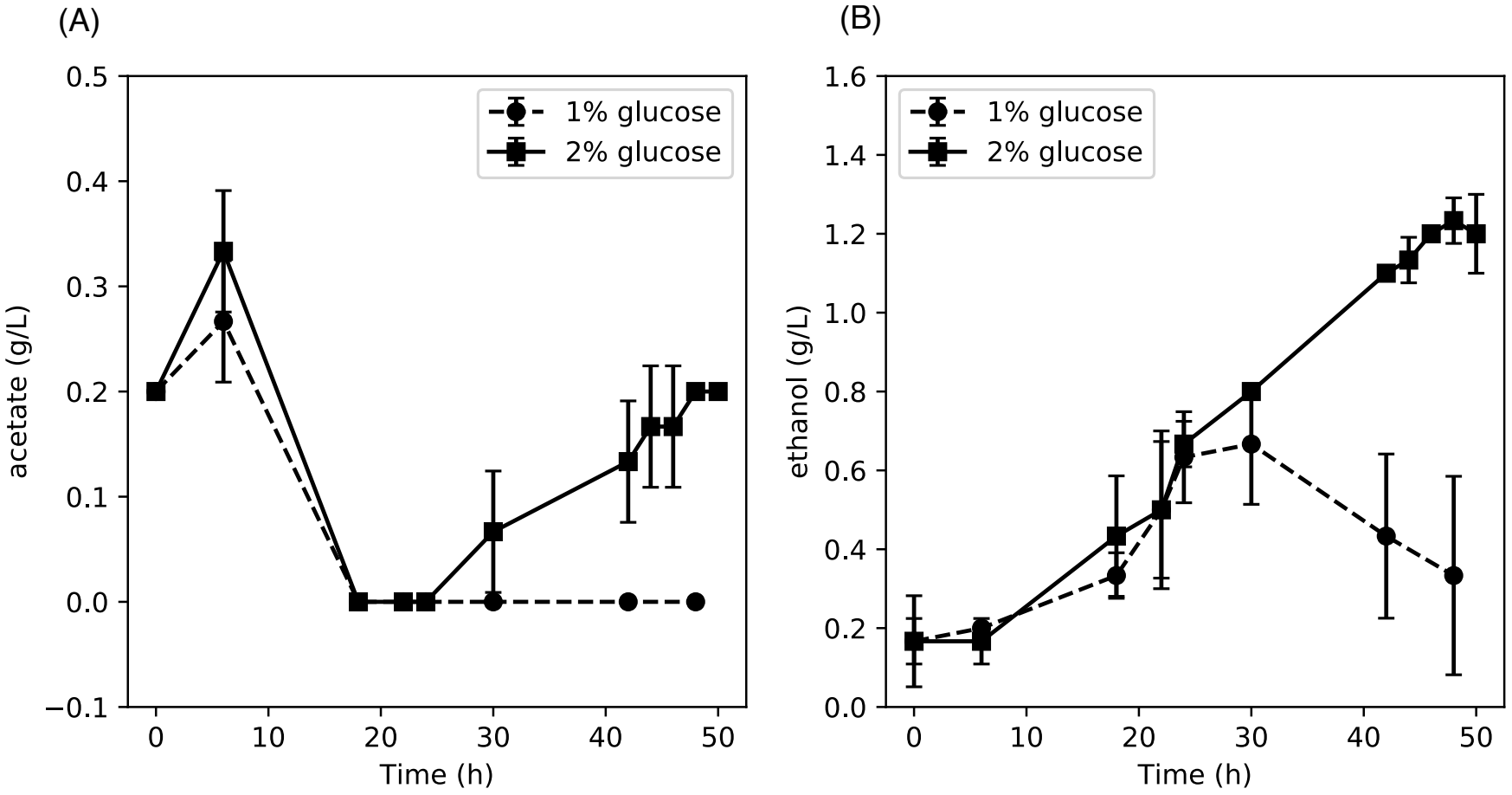

Supplementary Figure S5. Effect of NH_4Cl concentration on glucose consumption

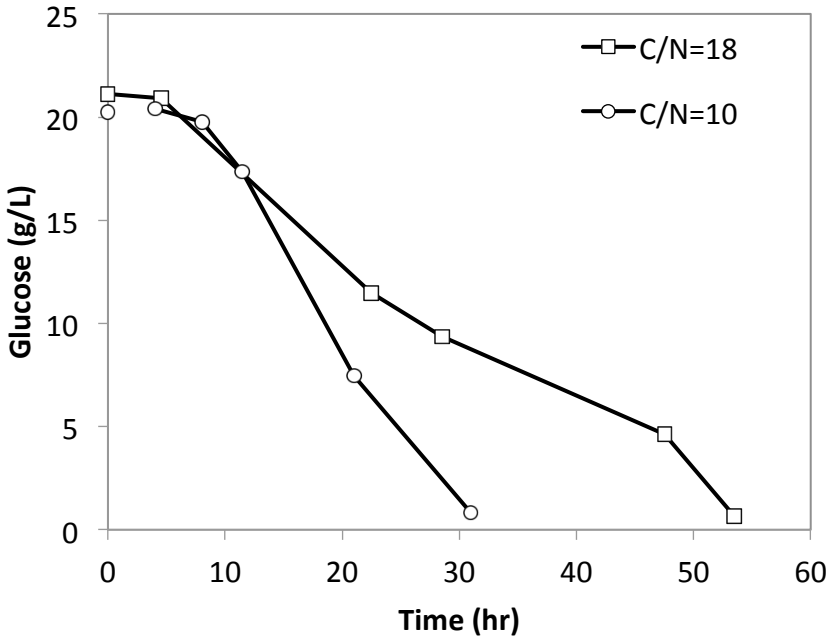

Supplementary Figure S6. Two phase fermentation. (A) comparison of dry cell weight (DCW); (B) glucose consumption; (C) distribution of isoprenol in the aqueous phase and oleyl alcohol phase at different time-points (Ferm 7); (D) isoprenol production in one-phase fermentation (Ferm 6). Ferm 6 corresponds to one-phase fermentation and Ferm 7 corresponds to two-phase fermentation

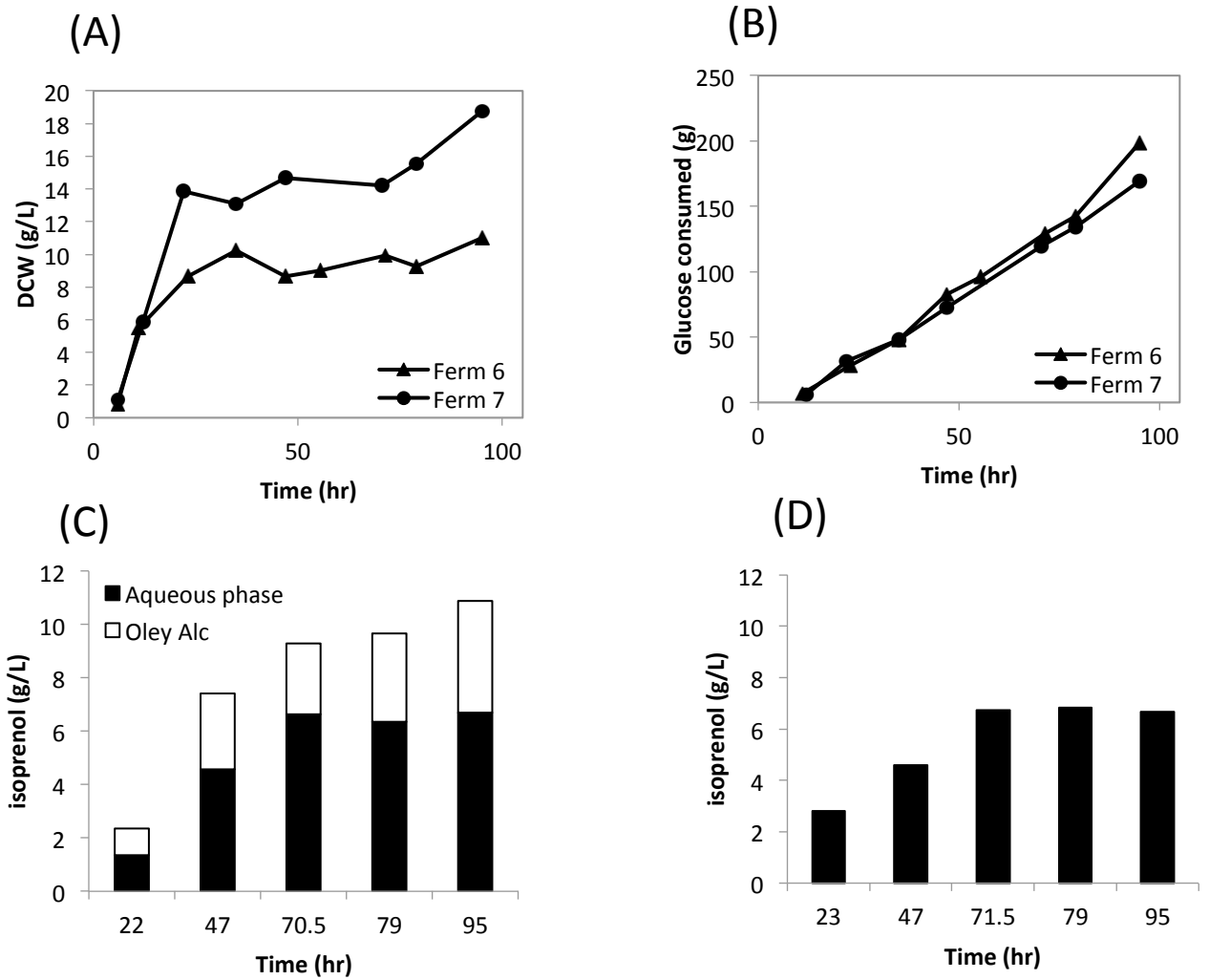

Supplementary Table S1: Titers, yields and maximum productivities for the different strains and fermentation conditions used in this study. Yield calculations correspond to the time at which the maximum titer was reached (grams of isopentenol /grams of glucose consumed). Productivity corresponds to the maximum productivity reached during the fermentation

Name	Strain	Batch medium	Feeding	Max Titer (g/L)	Yield (g/g)	Productivity ($g\ L^{-1}\ h^{-1}$)
Ferm 1	DH1	2% glucose, C/N=18	constant	3.55	0.048	0.031
Ferm 2	DH1	2% glucose, C/N=10	constant	3.44	0.054	0.040
Ferm 3	DH1	2% glucose, C/N=10	exponential	4.86	0.065	0.062
Ferm 4	DH1	2% glucose, yeast extract	exponential	5.42	0.069	0.079
Ferm 5	DH1 Δ*poxB* Δ*ackA-pta*	2% glucose, yeast extract	exponential	6.15	0.082	0.098
Ferm 6	DH1 Δ*poxB* Δ*ackA-pta*	3% glucose, yeast extract	exponential	6.84	0.073	0.121
Ferm 7	DH1 Δ*poxB* Δ*ackA-pta*	3% glucose, yeast extract, oleyl alcohol overlay	exponential	10.88	0.105	0.157